

Electronic Supplementary Information

Conducting Nanofibres of Solvatofluorochromic Cyclohexanetrione-Dithiolylidene-Based C_3 Symmetric Molecule

Kilingaru I. Shivakumar,^{a,b} Goudappagouda,^{a,b} Rajesh Gonnade,^{b,c} Sukumaran Santhosh Babu,^{*a,b} Gangadhar J. Sanjayan^{*a,b}

^aDivision of Organic Chemistry, ^bAcademy of Scientific and Innovation Research, ^cCentre for Materials Characterization

CSIR-National Chemical Laboratory, Dr. Homi Bhabha Road, Pashan, Pune 411 008, INDIA

Table of Contents

1. General methods	page S2-S3
2. Synthesis and characterization: scheme, experimental procedure and characterization data (NMR and mass spectra)	pages S4-S30
3. Absorption, emission spectra and lifetime measurements	page S31
4. Cyclic voltammetry	page S32
5. Crystal structure data and packing	pages S34-S35
6. Microscopic images of self-assembled structures	Pages S36-S38
7. Nanofibre characterization – powder XRD, solid-state absorption and emission spectra and cyclic voltammetry	Pages S39-S43
7. Conductivity	Page S44-S7
8. References	Page S47

1. General methods

All the chemicals used as starting materials and reagents were purchased from commercial suppliers. Triethylamine and acetonitrile were dried according to the standard procedures. Analytical Thin Layer Chromatography (TLC) was carried out on precoated silica gel plates (Kieselgel 60F₂₅₄, Merck). Column chromatographic purifications were performed using 230-400 mesh silica gel.

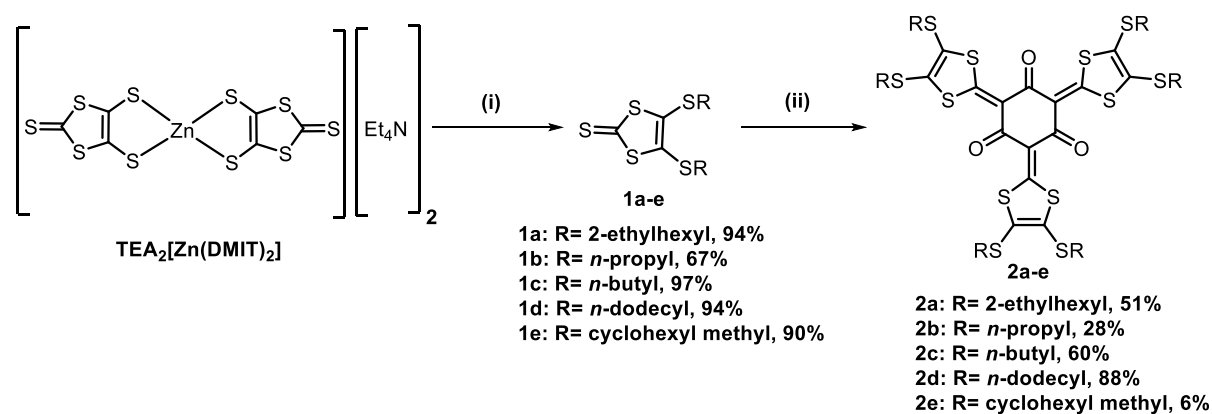
NMR spectra were recorded in CDCl₃ on AV 400 and 500 MHz Bruker NMR spectrometers. Chemical shifts are reported in δ ppm, and downfield to TMS with peak multiplicities mentioned as singlet (s), doublet (d), triplet (t), quartet (q) and multiplet (m) in ¹H NMR spectra. IR spectra were recorded as a solution in chloroform using Bruker alpha platinum ATR spectrophotometer. Melting points were determined on a Buchi Melting Point B-540 and are uncorrected. High resolution mass spectroscopy (HRMS) measurements were recorded using Thermo Scientific Q-Exactive, Accela 1250 pump mass spectrometer. The poor solubility of the alkyl chain appended compounds **1c-e** and **2a-d** in acetonitrile and methanol precluded us from obtaining satisfactory HRMS. Hence, these compounds were subjected to MALDI-TOF/TOF measurements employing ABSCIEX TOF/TOFTM 5800 mass spectrometer.

Absorption spectra were recorded in shimadzu 1800 spectrophotometer. Emission spectra were collected using PTI Quanta MasterTM steady state spectrofluorometer. Fluorescence lifetimes were measured by time correlated single photon counting (TCSPC), employing a spectrofluorometer (Horiba scientific) and LED excitation source of 443 nm. The quality of the fit has been judged by the fitting parameters such as χ^2 (<1.2) and also by the visual inspection of the residuals. Optical microscopy images of the self-assembly were obtained using Zeta instruments' optical microscope possessing 5x, 10x and 20x objective lens. SEM images were obtained using FEI, QUANTA 200 3D scanning electron microscope operating at 10, 15 and 20 kV using tungsten filament as electron source. Prior to imaging, the samples were sputtered with gold by using SCD 040 Balzers Union sputterer. FEI Tecnai G2 F20 XTWIN TEM with accelerating voltage of 200 kV was used for the TEM imaging, 200 mesh TEM copper grids were purchased from TED PELLA, INC. The wide-angle X-ray diffraction measurements were performed using a Rigaku Micromax-007HF diffractometer operating at 40 kV and 30 mA. The sample was exposed to the X-ray beam for 3 minutes and the

scattering pattern was imaged by Rigaku R-Axis IV++ area detector. The conversion from 2D pattern to 1D was done using Rigaku 2DP software.

Cyclic voltammetry experiments were performed using CH instruments electrochemical workstation (solution) and Versa Stat 3 (Princeton Applied Research) instrument (nanofibre). The experiments were carried out employing glassy carbon, platinum and Ag/AgCl as working, counter and reference electrodes, respectively and Bu_4NPF_6 (0.1 M) as supporting electrolyte at a scan rate of 50 mVs^{-1} . HOMO and LUMO energy levels are calculated from the onset of first oxidation and reduction waves using the formulae $\text{HOMO} = -(E_{\text{ox}} + 4.4)$ and $\text{LUMO} = -(E_{\text{red}} + 4.4)$. Bruker multimode 8.0 was used to obtain atomic force microscopy (AFM) images and to measure the conductivity (current-sensing AFM). AFM images were recorded in tapping mode using silicon nitride cantilever tip, having a thickness of 650 nm, length of $115 \mu\text{m}$ and width of $25 \mu\text{m}$, and operating at a resonance frequency of 70 kHz with a spring constant of 0.4 Nm^{-1} . AFM section analysis was carried out offline using SPIP 6.7.1 program. Conductivity measurements were executed at ambient conditions employing the same instrument with antimony doped silicon cantilever tip possessing resistivity of $0.01 - 0.025 \Omega\text{cm}$, having a thickness of $2.5 - 3.5 \mu\text{m}$, length of $200 - 250 \mu\text{m}$, width $23 - 33 \mu\text{m}$, and operating at a resonance frequency of $60 - 100 \text{ kHz}$ and a spring constant of $1 - 5 \text{ Nm}^{-1}$.

Scheme 1. Synthesis of compounds **2a-e**



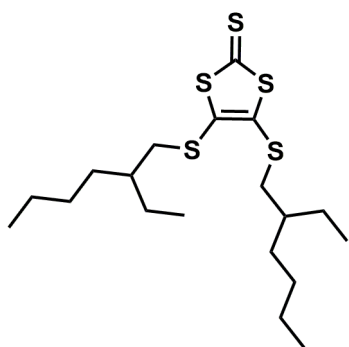
Reagents and Conditions: (i) RBr, MeCN, reflux, 2 h; (ii) phloroglucinol, **1a-e**, Et₃N, AgNO₃, MeCN, 75 °C, 12 h.

Synthesis of bis(tetraethylammonium)bis(1,3-dithiole-2-thione-4,5-dithiolato) zincate $\text{TEA}_2[\text{Zn}(\text{DMIT})_2]$

The deep red organometallic complex $\text{TEA}_2[\text{Zn}(\text{DMIT})_2]$ was synthesized according to the reported procedure.¹

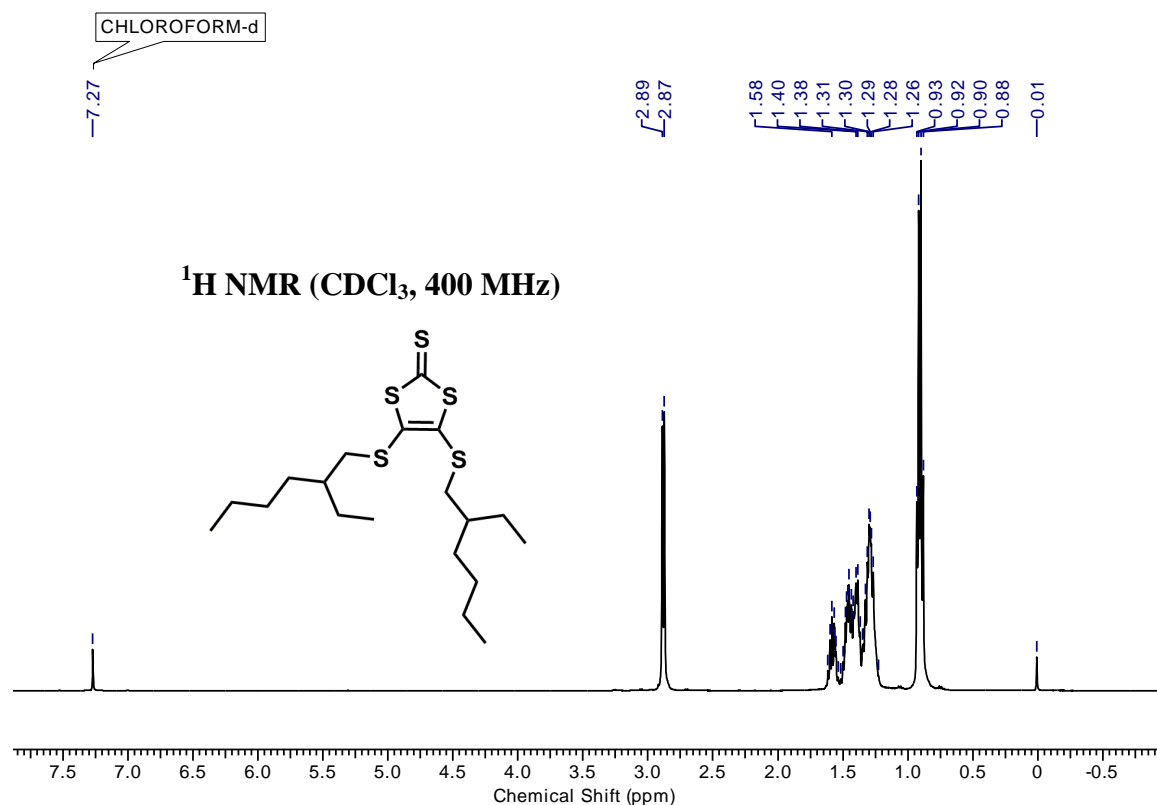
Synthesis of compounds 4,5-bis(alkylthio)-1,3-dithiole-2-thiones (1a-1e)

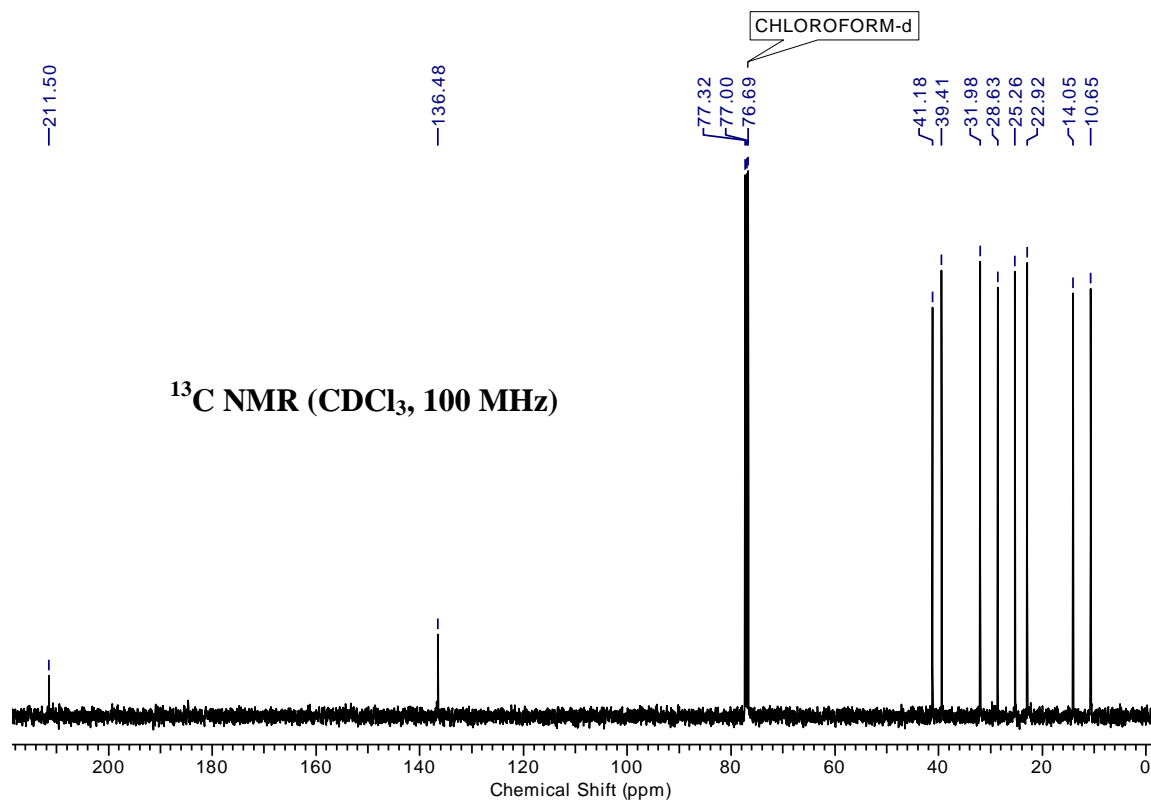
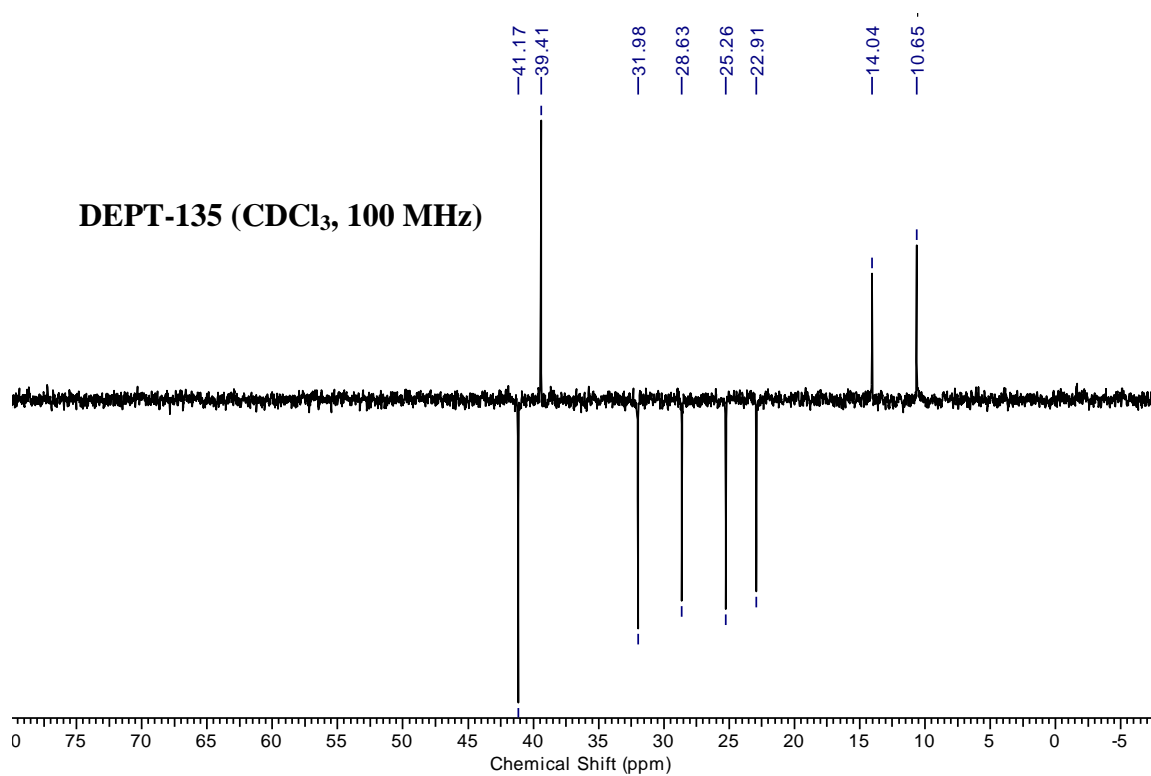
Representative procedure for 4,5-bis((2-ethylhexyl)thio)-1,3-dithiole-2-thione (**1a**)

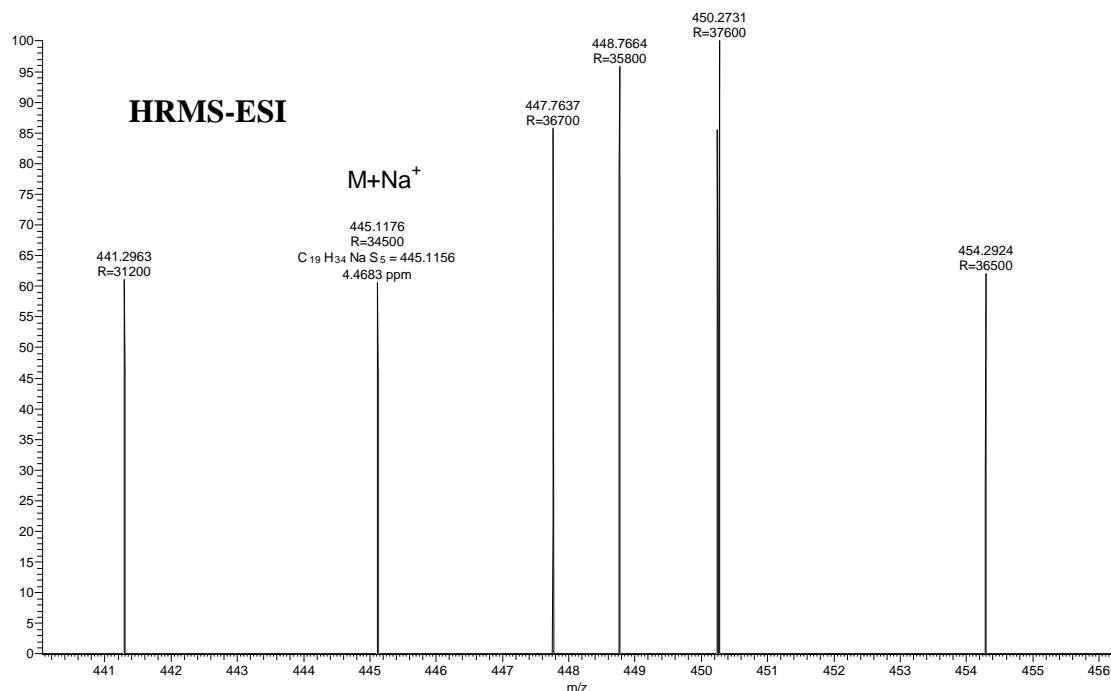


To the solution of $\text{TEA}_2[\text{Zn}(\text{DMIT})_2]$ (300 mg, 0.42 mmol) in acetonitrile (10 mL), 2-ethylhexyl bromide (297 mg, 1.67 mmol) was added and the reaction mixture was refluxed for 2 h. The reaction mixture, after being cooled to room temperature, was filtered. The filtrate was concentrated *in vacuo* and purified by column chromatography (eluent: petroleum ether, $R_f = 0.2$) to furnish **1a** as brown oil (240 mg, 94%); IR (CHCl_3) ν (cm^{-1}):

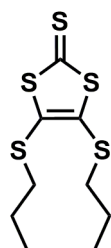
2962, 2930, 2861, 1601, 1522, 1464, 1426, 1064, 929, 851; ^1H NMR (400 MHz, chloroform-*d*) $\delta = 2.88$ (d, $J = 6.1$ Hz, 4H), 1.64 - 1.53 (m, 2H), 1.52 - 1.36 (m, 8H), 1.36 - 1.20 (m, 8H), 0.98 - 0.81 (m, 12H); ^{13}C NMR (100 MHz, chloroform-*d*) $\delta = 211.5$, 136.5, 41.2, 39.4, 32.0, 28.6, 25.3, 22.9, 14.0, 10.7; HRMS: $\text{C}_{19}\text{H}_{34}\text{NaS}_5$ ($\text{M}+\text{Na}$)⁺ Calcd: 445.1156, found: 445.1176



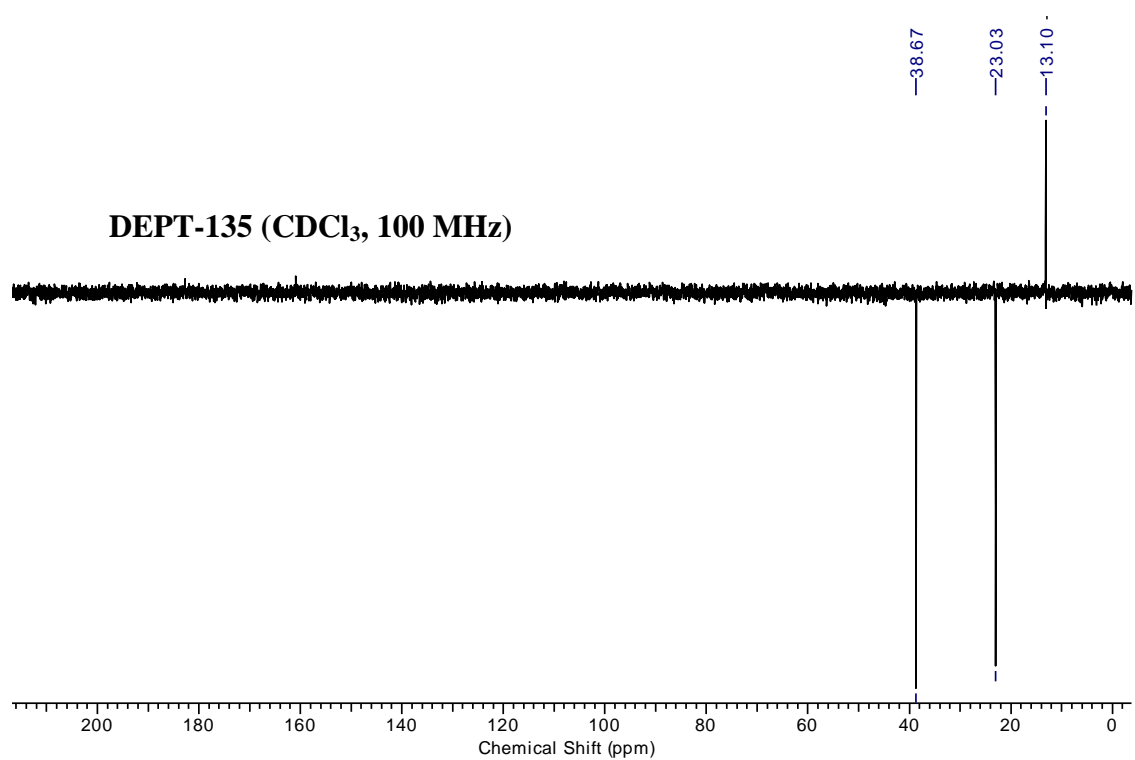
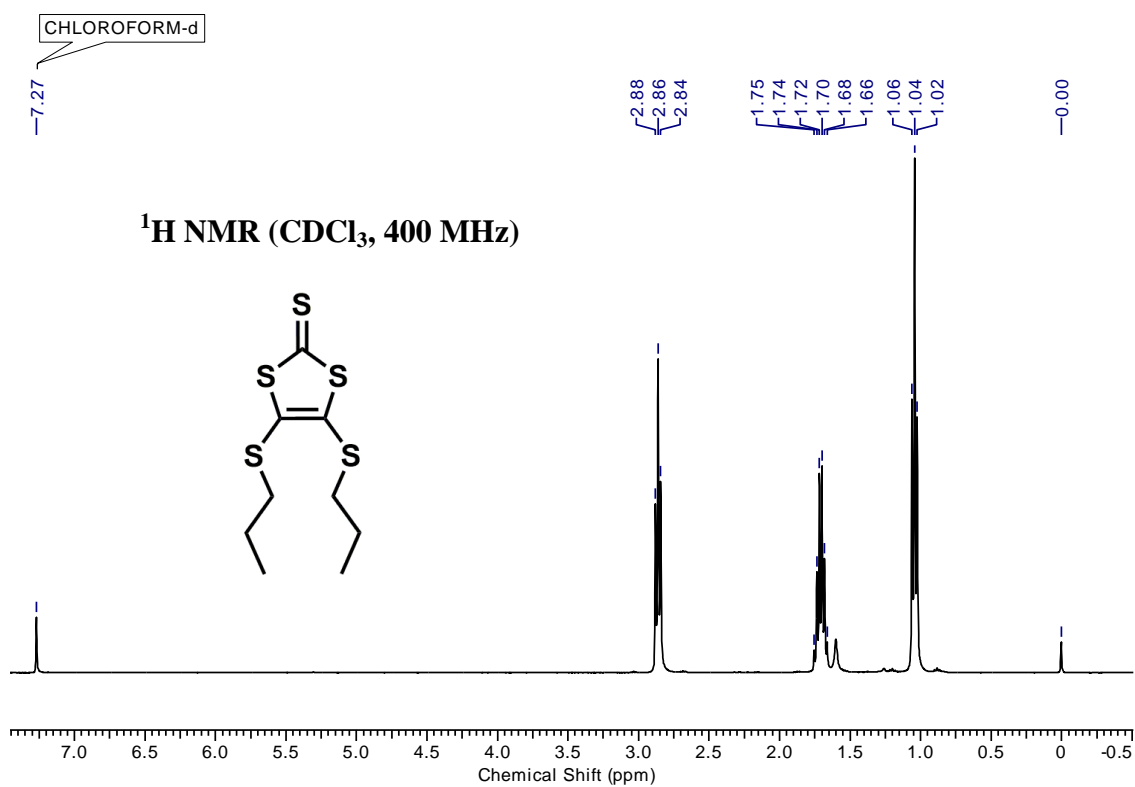


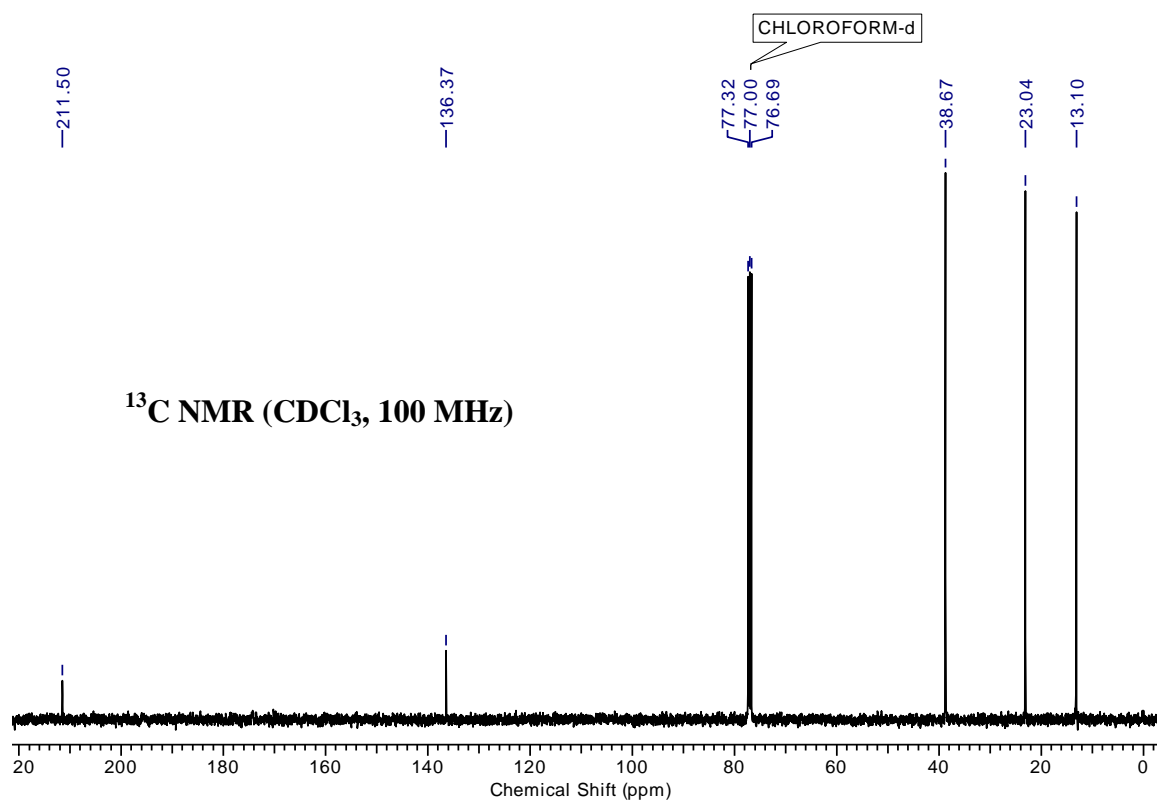


4,5-bis(propylthio)-1,3-dithiole-2-thione (**1b**)

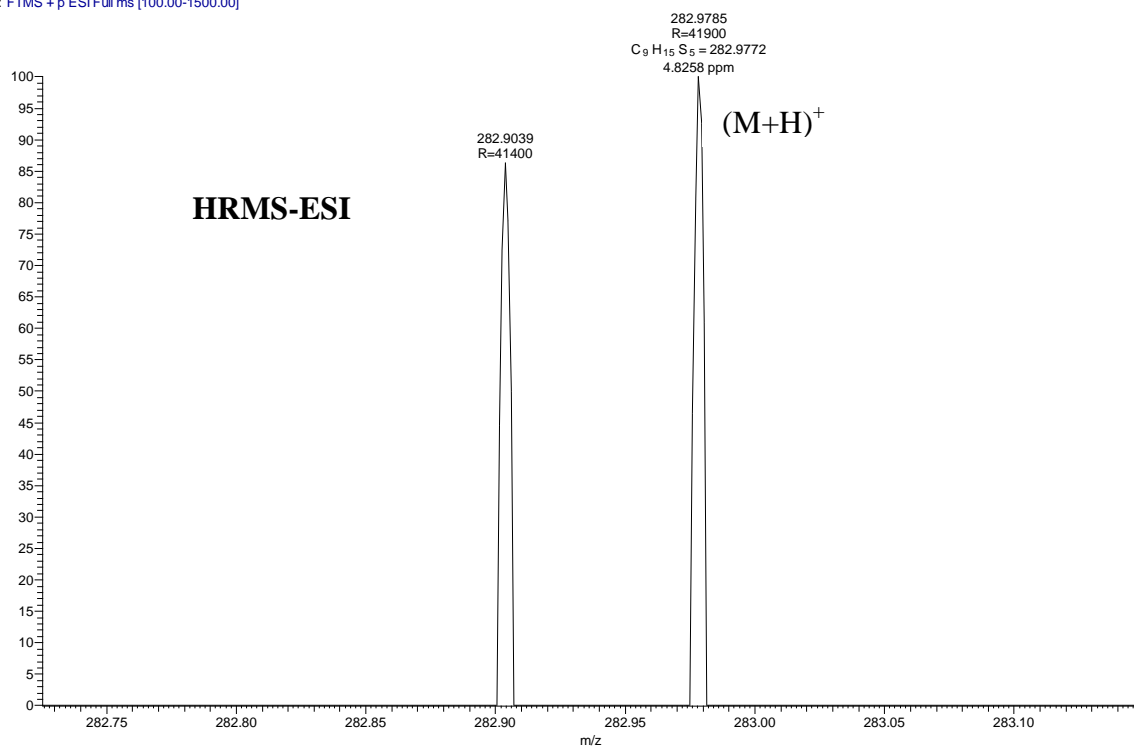


The compound **1b** was obtained following the same procedure employed for **1a** using TEA₂[Zn(DMIT)₂] (200 mg, 0.28 mmol) and propyl bromide (127 μ L, 1.4 mmol). Column chromatography (eluent: petroleum ether, R_f = 0.35) furnished compound **1b** as brown oil (105 mg, 67%); IR (CHCl₃) ν (cm⁻¹): 1601, 1524, 1424, 1064, 928, 909; ¹H NMR (400MHz, chloroform-*d*) δ = 2.86 (t, J = 7.3 Hz, 4H), 1.87 - 1.63 (m, 4H), 1.04 (t, J = 7.3 Hz, 6H); ¹³C NMR (100 MHz, chloroform-*d*) δ = 211.5, 136.4, 38.7, 23.0, 13.1; HRMS: C₉H₁₅S₅ (M+H)⁺ calcd: 282.9772, found: 282.9785.

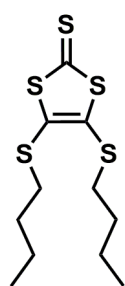




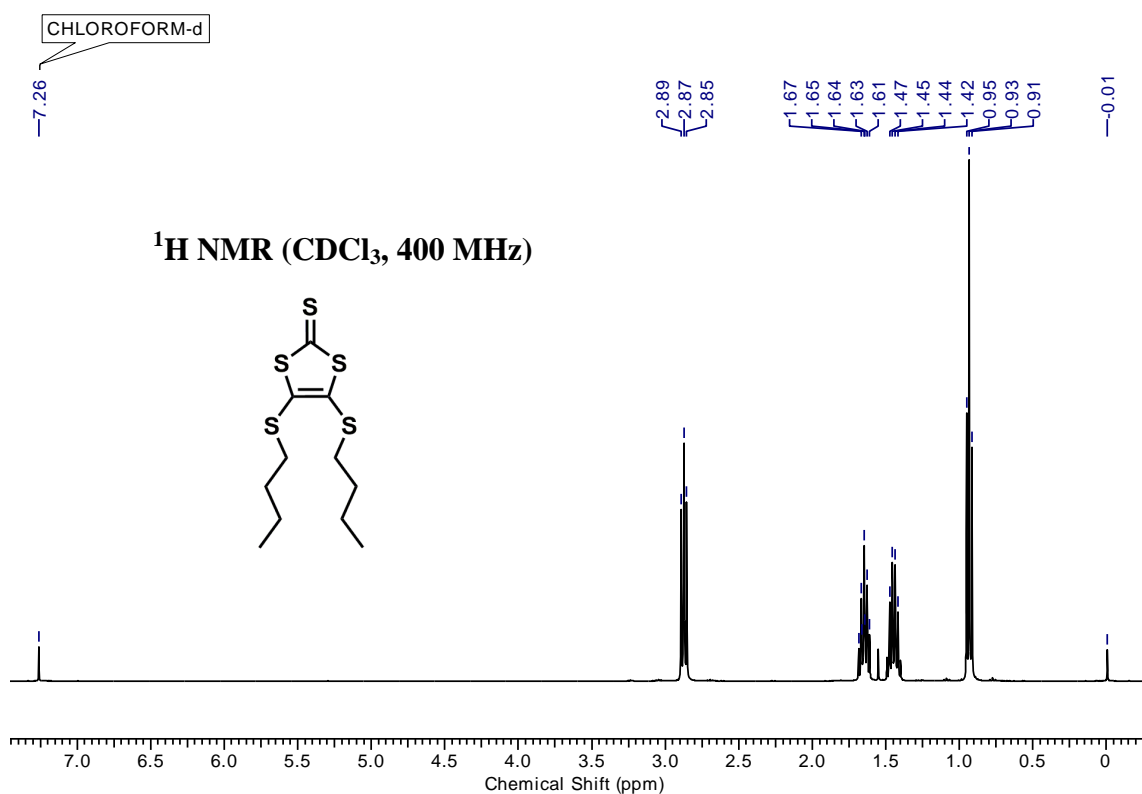
PROPYL-THIONE #146 RT: 0.65 AV: 1 NL: 5.44E4
T: FTMS + p ESI Full ms [100.00-1500.00]

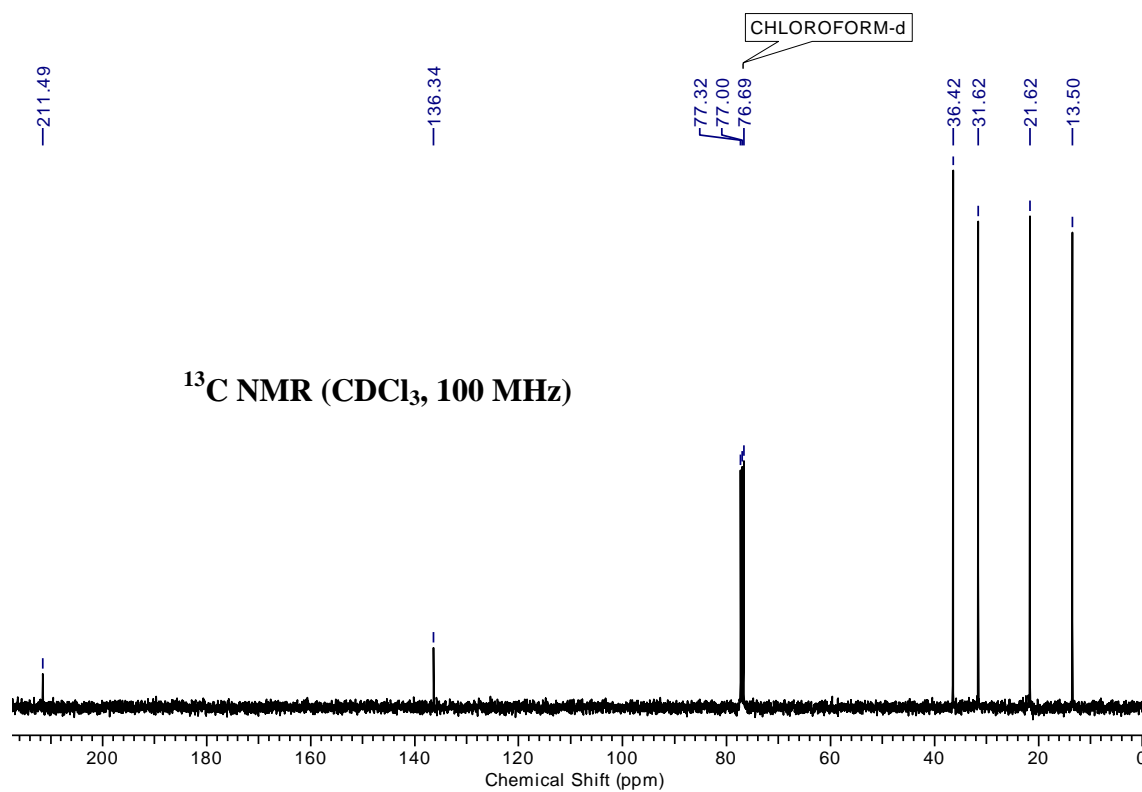
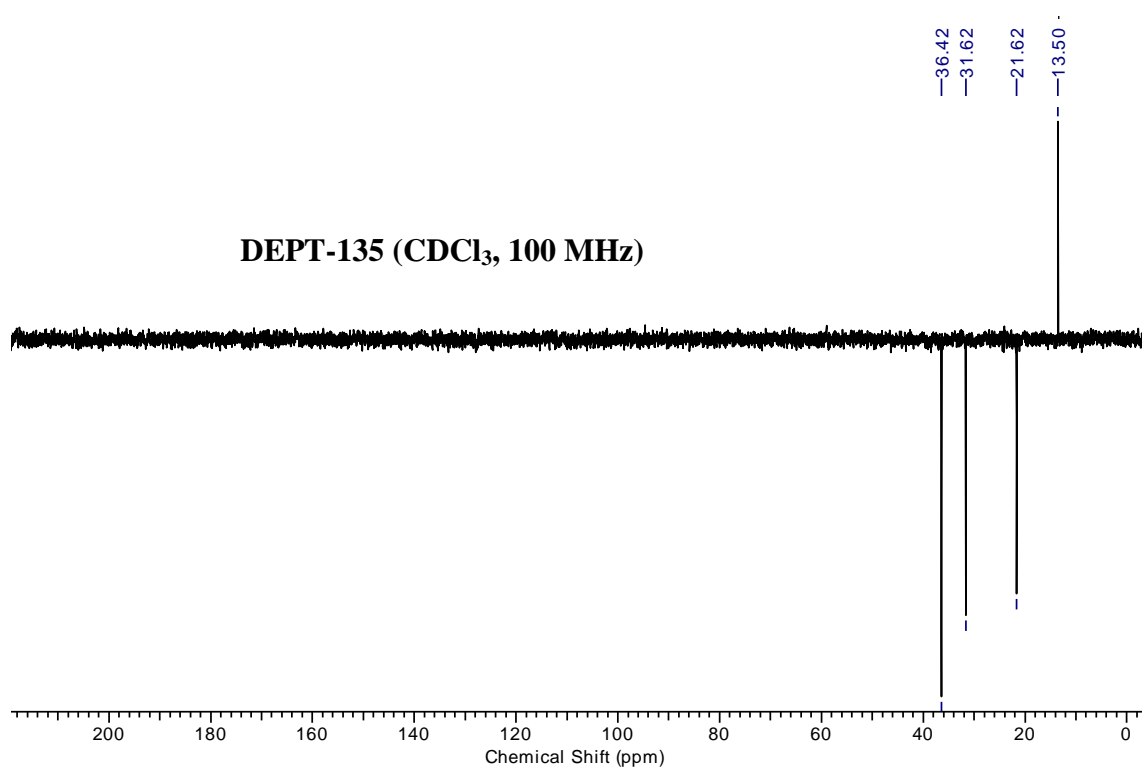


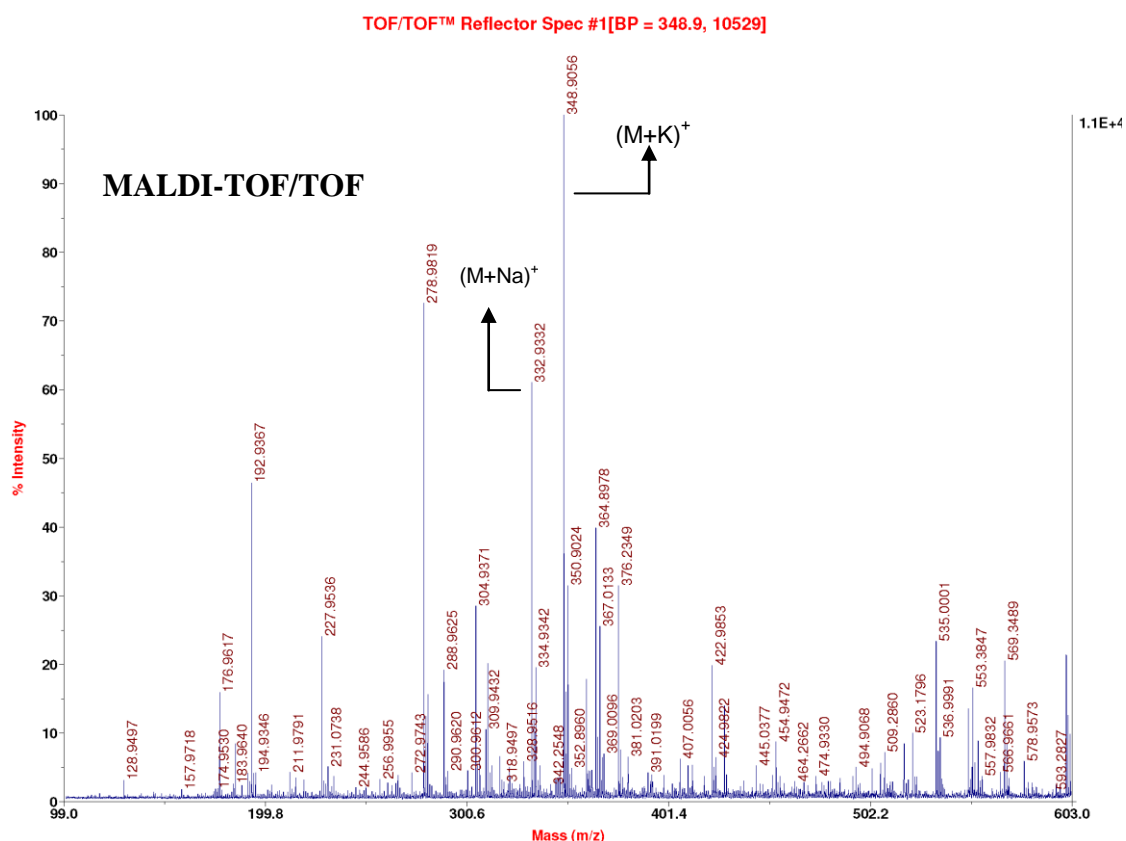
4,5-bis(butylthio)-1,3-dithiole-2-thione (**1c**)



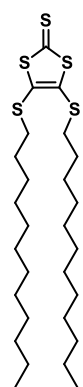
The compound **1c** was obtained following the same procedure employed for **1a** using TEA₂[Zn(DMIT)₂] (500 mg, 0.70 mmol) and butyl bromide (374 μ L, 3.49 mmol). Column chromatography (eluent: petroleum ether, R_f = 0.65) furnished compound **1c** as brown oil (421 mg, 97%); IR (CHCl₃) ν (cm⁻¹): 2963, 2933, 2875, 1601, 1523, 1466, 1065, 929; ¹H NMR (400 MHz, chloroform-*d*) δ = 2.91 - 2.83 (m, 4H), 1.70 - 1.60 (m, 4H), 1.51 - 1.39 (m, 4H), 0.93 (t, J = 7.5 Hz, 6H); ¹³C NMR (100 MHz, chloroform-*d*) δ = 211.5, 136.3, 36.4, 31.6, 21.6, 13.5; MALDI-TOF/TOF: 332.93 (M+Na)⁺, 348.91 (M+K)⁺.



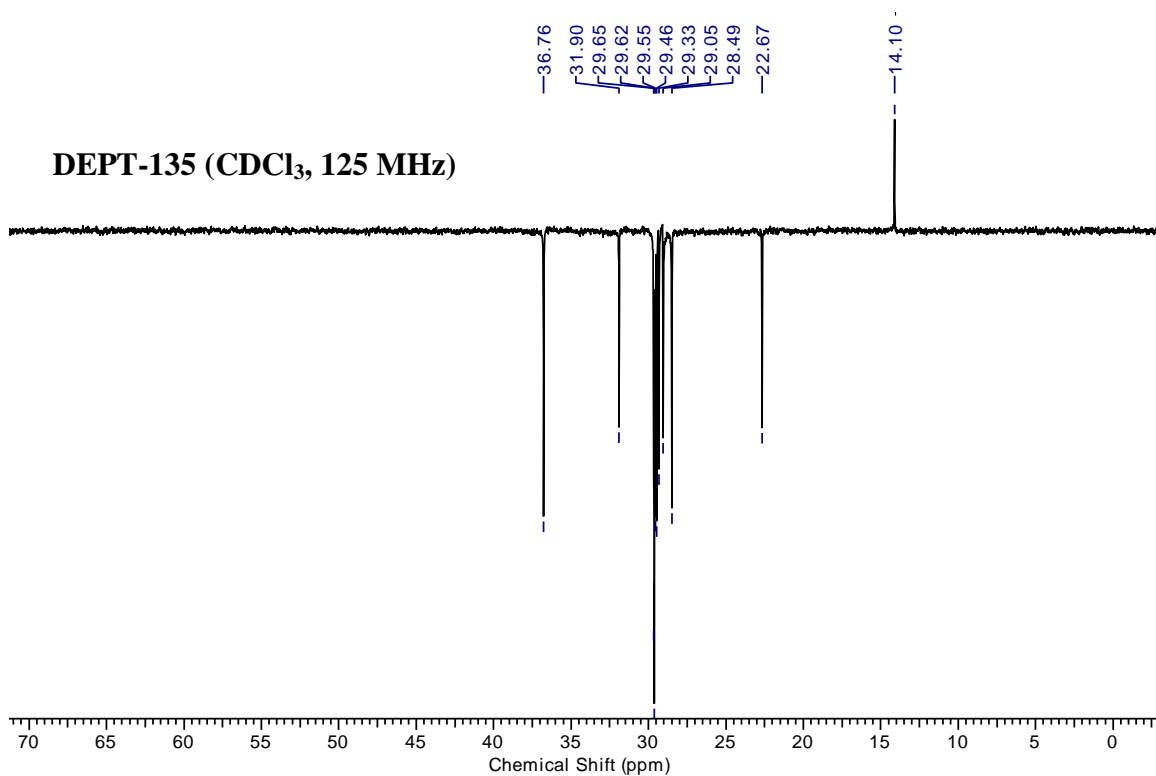
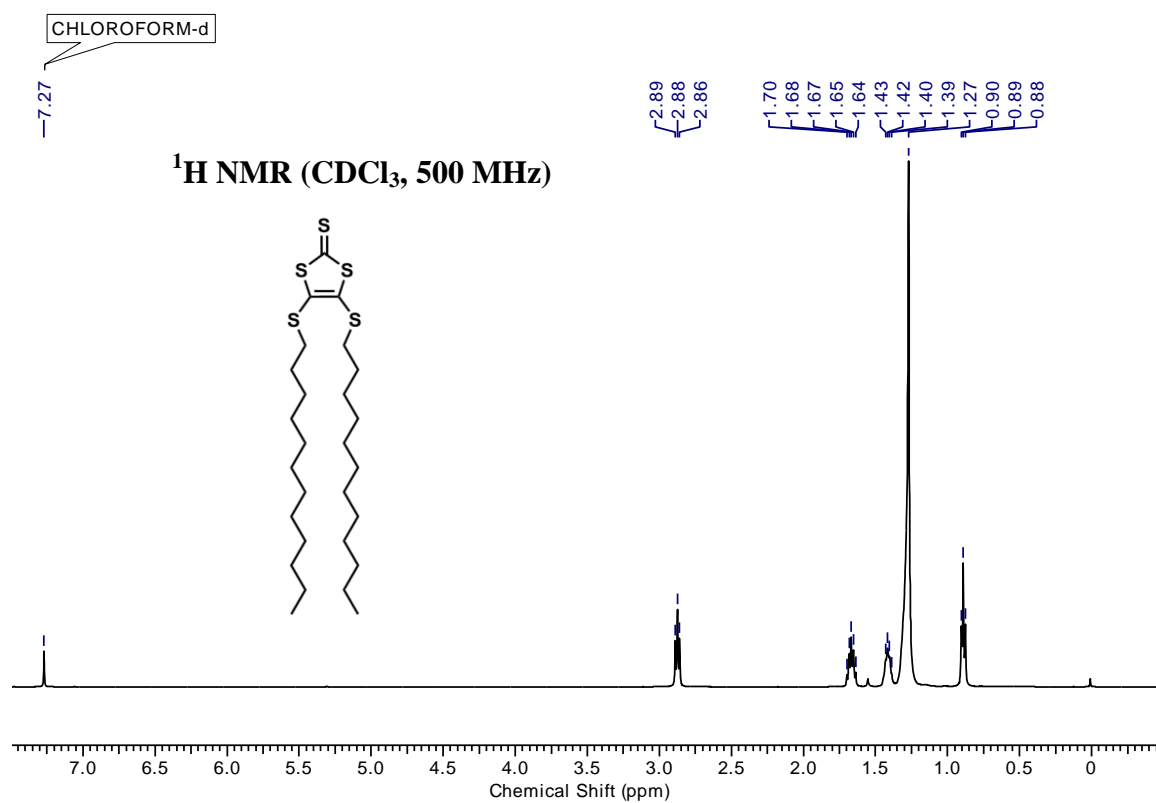


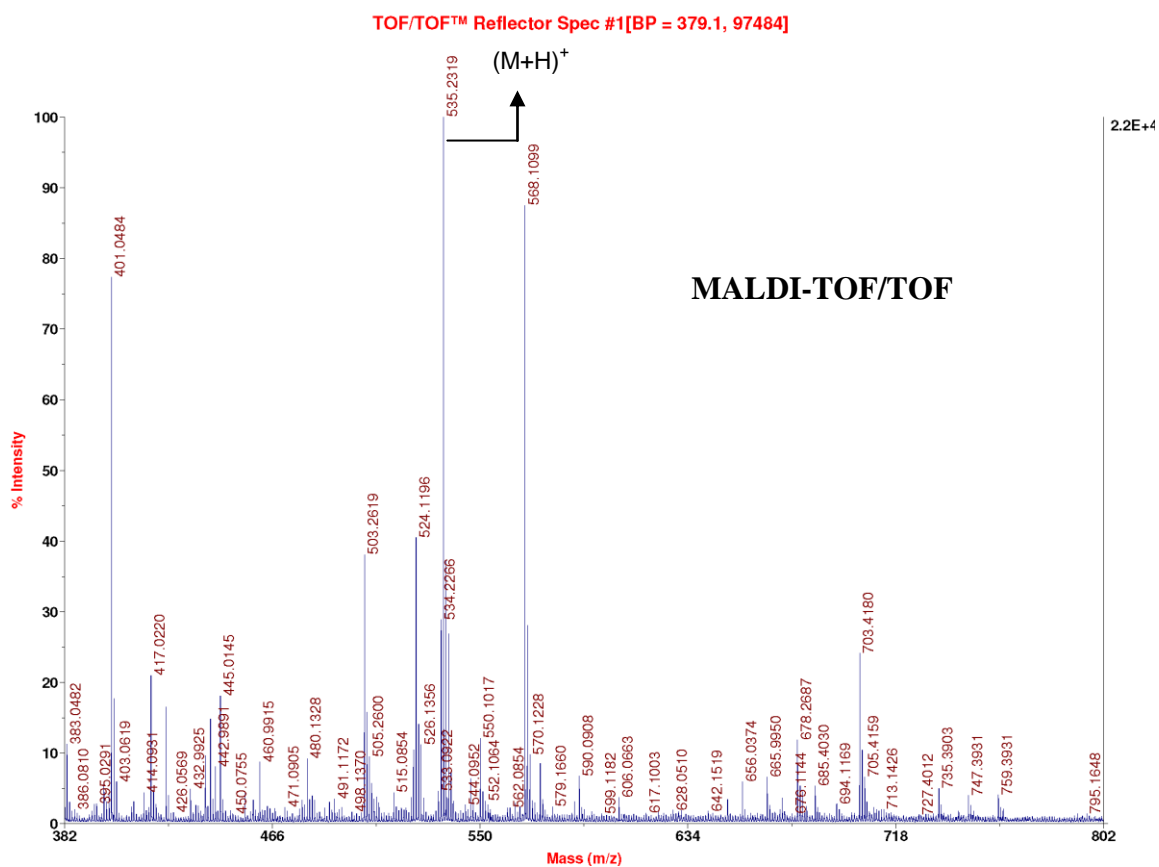
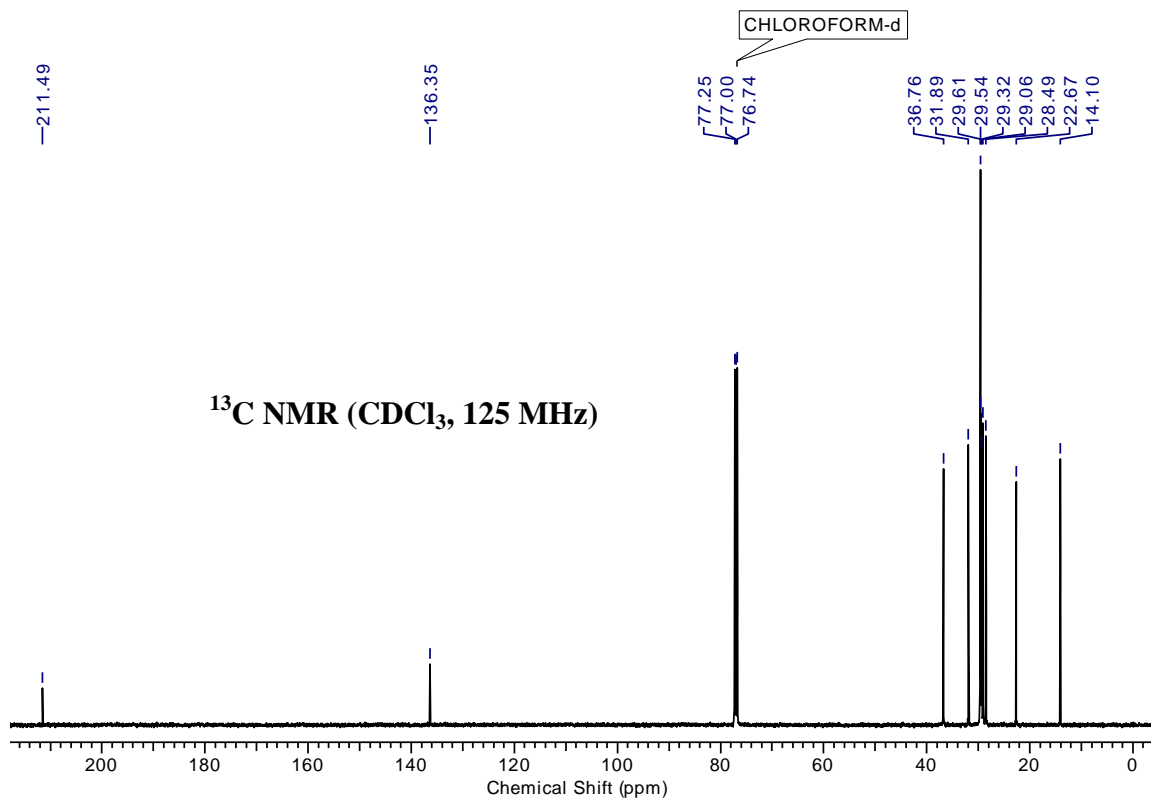


4,5-bis(dodecylthio)-1,3-dithiole-2-thione (**1d**)

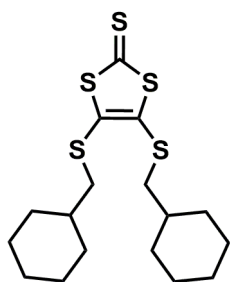


The compound **1d** was obtained following the same procedure employed for **1a** using TEA₂[Zn(DMIT)₂] (500 mg, 0.70 mmol) and dodecyl bromide (835 μL, 3.48 mmol). Column chromatography (eluent: petroleum ether, *R_f* = 0.65) furnished compound **1d** as yellow solid (698 mg, 94%); mp: 52-53 °C; IR (CHCl₃) *v* (cm⁻¹): 2928, 2855, 1601, 1525, 1465, 1425, 1065, 929, 851; ¹H NMR (500 MHz, chloroform-*d*) *δ* = 2.87 (t, *J* = 7.4 Hz, 4H), 1.67 (quin, *J* = 7.4 Hz, 4H), 1.47 - 1.37 (m, 4H), 1.27 (br. s., 32H), 0.89 (t, *J* = 6.9 Hz, 6H); ¹³C NMR (125 MHz, chloroform-*d*) *δ* = 211.5, 136.3, 36.8, 31.9, 29.6, 29.6, 29.5, 29.5, 29.3, 29.1, 28.5, 22.7, 14.1; MALDI-TOF/TOF: 535.23 (M+H)⁺

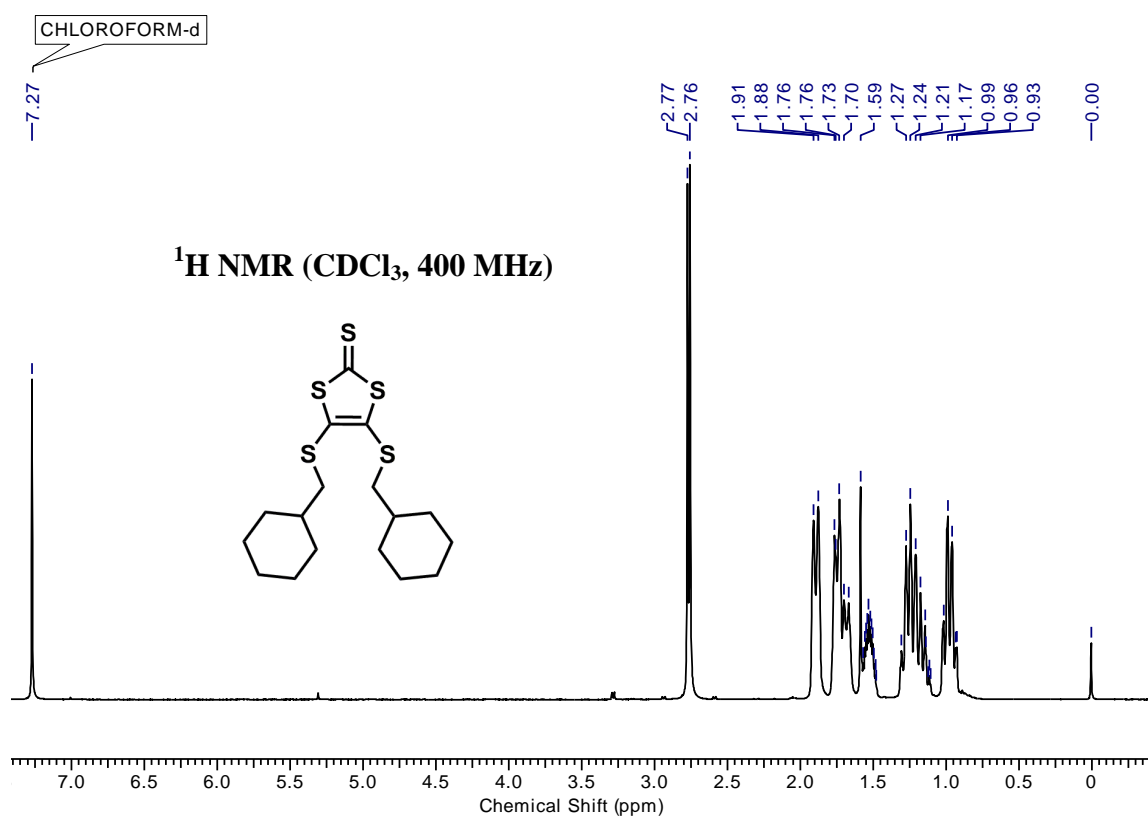


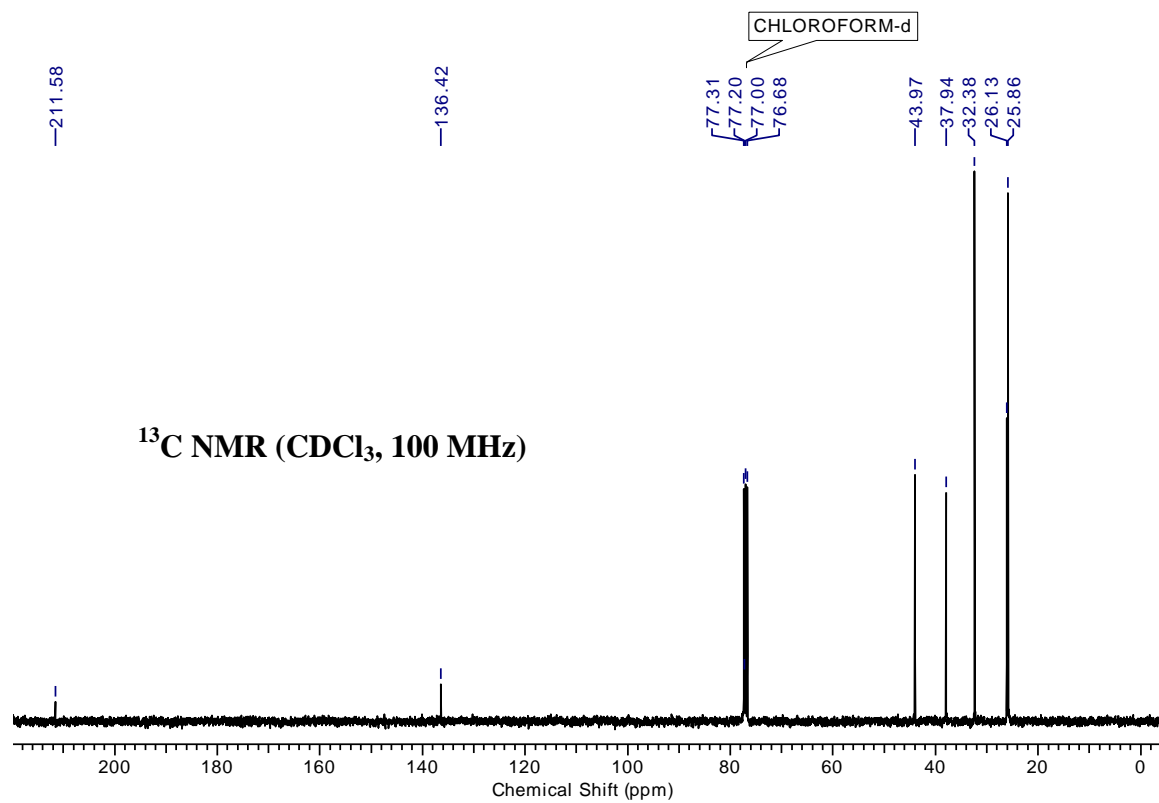
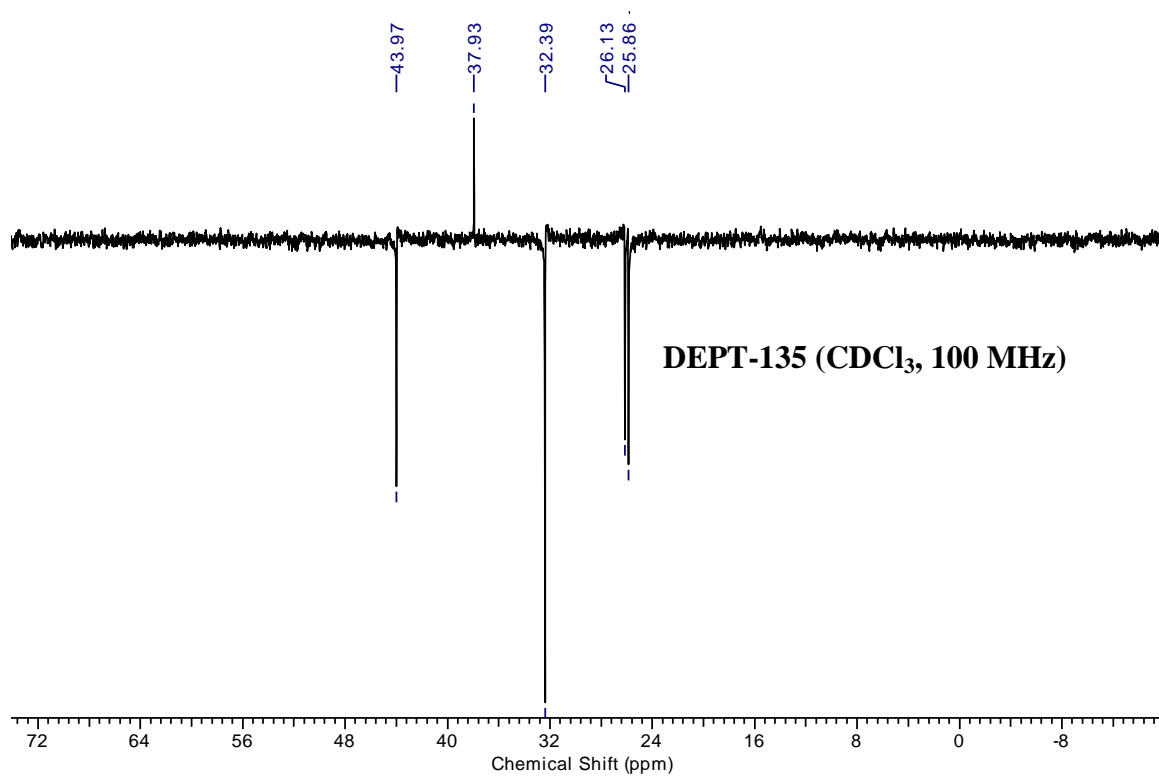


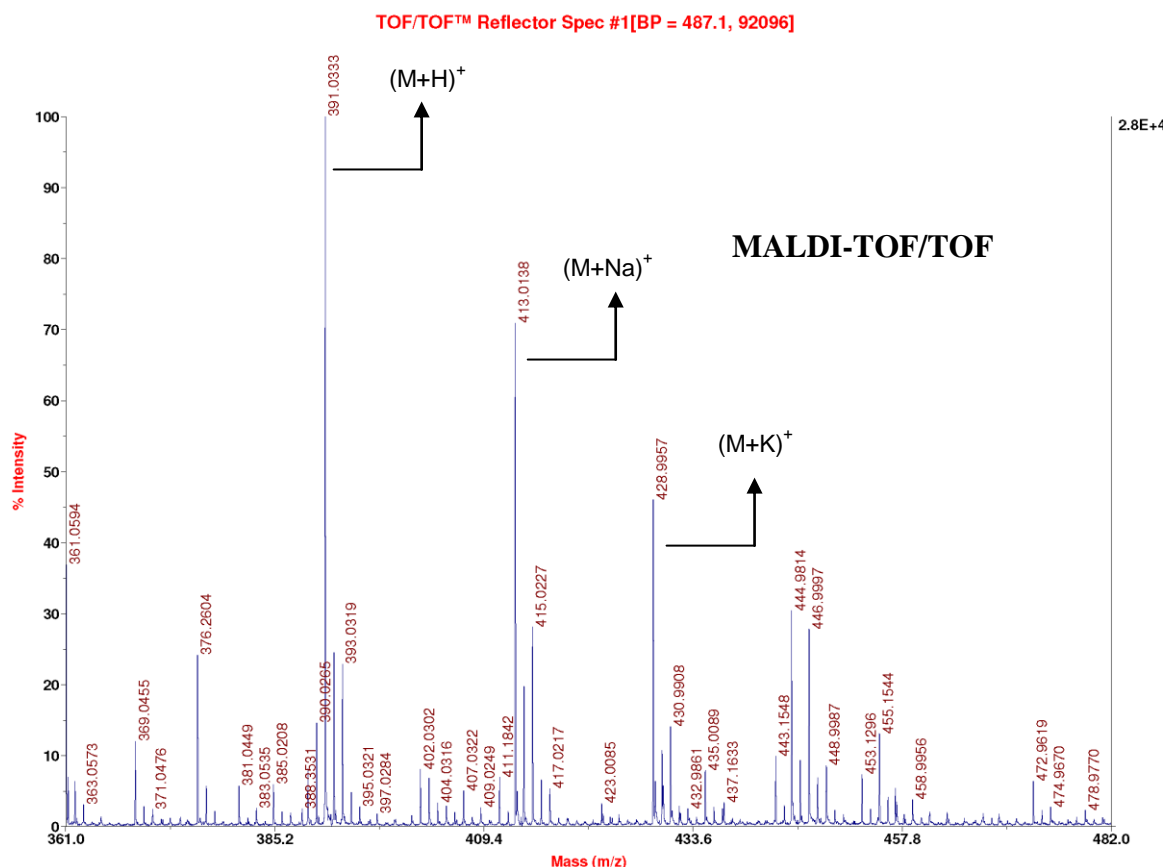
4,5-bis((cyclohexylmethyl)thio)-1,3-dithiole-2-thione (**1e**)



The compound **1e** was obtained following the same procedure employed for **1a** using $\text{TEA}_2[\text{Zn}(\text{DMIT})_2]$ (200 mg, 0.28 mmol) and cyclohexylmethyl bromide (296 mg, 1.67 mmol). Purification was carried out using column chromatography (eluent: petroleum ether, $R_f = 0.2$) to furnish **1e** as brown oil (195 mg, 90%); IR (CHCl_3) ν (cm^{-1}): 2923, 2850, 1630, 1307, 1067, 1032, 961, 890; ^1H NMR (400MHz, chloroform-*d*) δ = 2.76 (d, J = 6.7 Hz, 4H), 1.89 (d, J = 12.2 Hz, 4H), 1.80 - 1.71 (m, 4H), 1.67 (br. s., 2H), 1.57 - 1.46 (m, 2H), 1.33 - 1.09 (m, 6H), 1.05 - 0.91 (m, 4H); ^{13}C NMR (100 MHz, chloroform-*d*) δ = 211.6, 136.4, 44.0, 37.9, 32.4, 26.1, 25.9; MALDI-TOF/TOF: 391.03 ($\text{M}+\text{H}$) $^+$, 413.01 ($\text{M}+\text{Na}$) $^+$, 428.99 ($\text{M}+\text{K}$) $^+$.

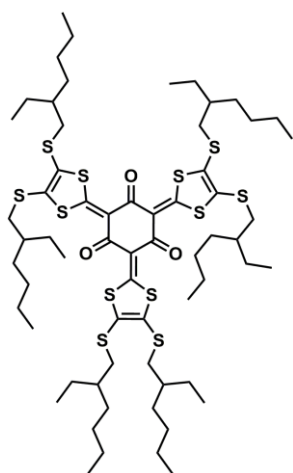






Synthesis of compounds 2,4,6-tris(4,5-bis(alkylthio)-1,3-dithiol-2-ylidene)cyclohexane-1,3,5-triones (2a-e)

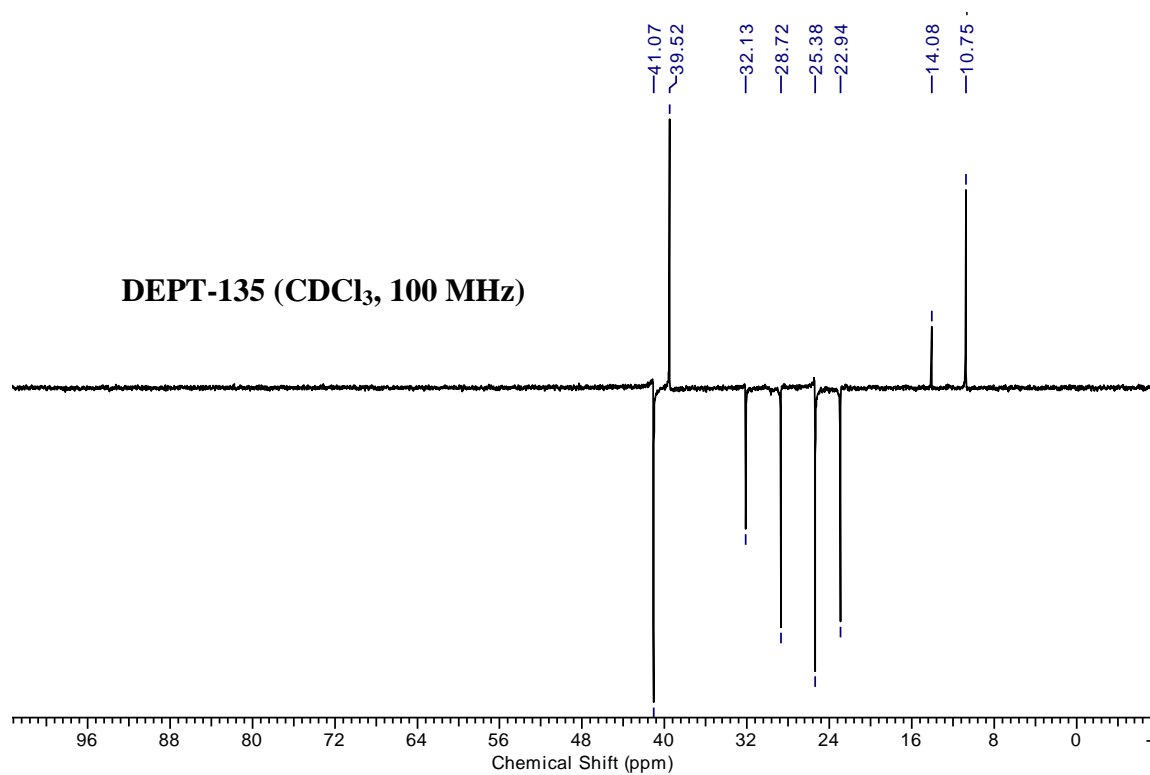
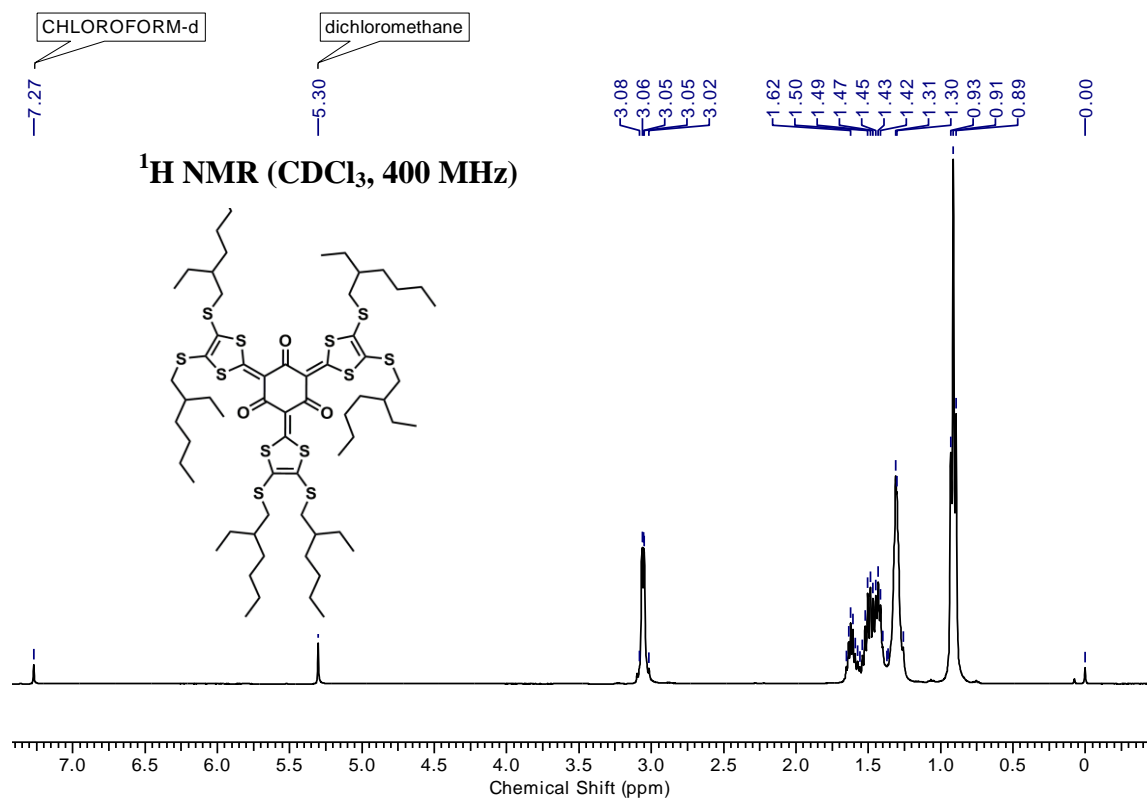
Representative procedure for **2,4,6-tris(4,5-bis((2-ethylhexyl)thio)-1,3-dithiol-2-ylidene)cyclohexane-1,3,5-trione (2a)**

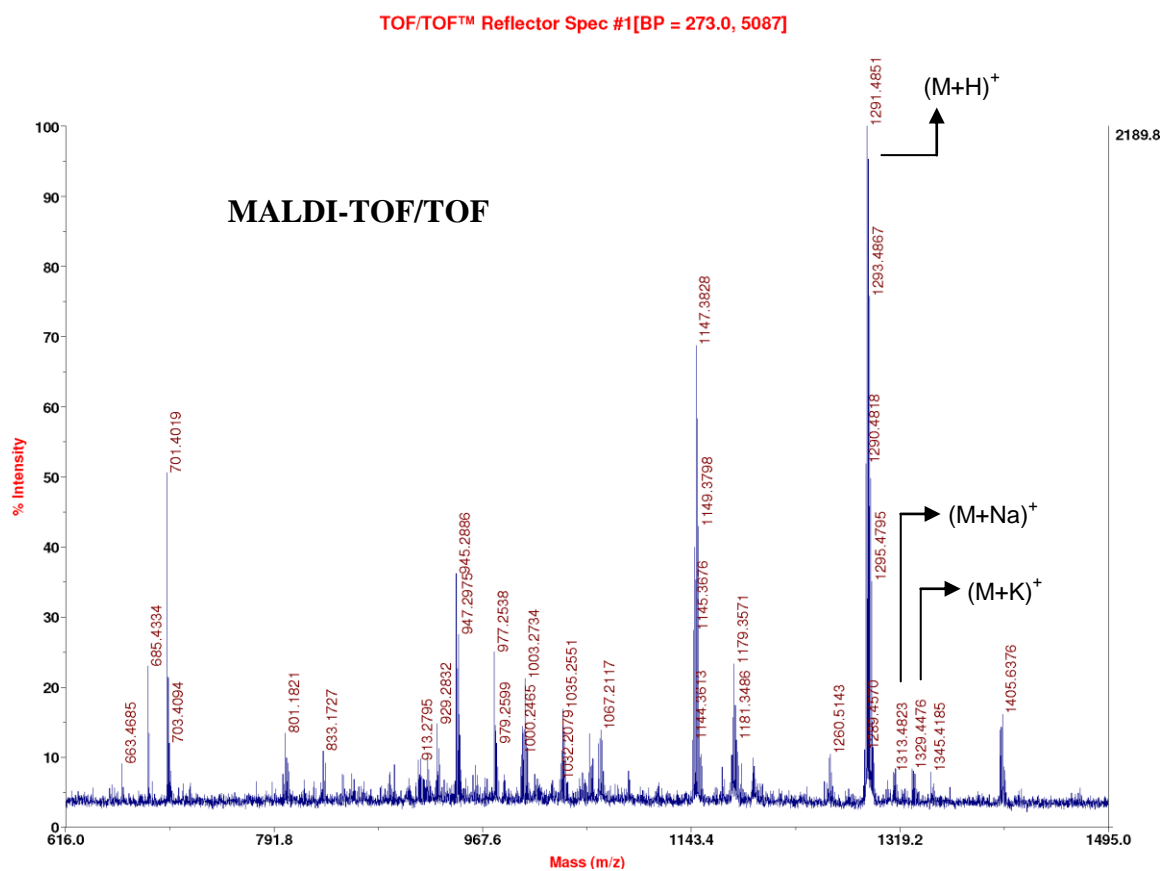
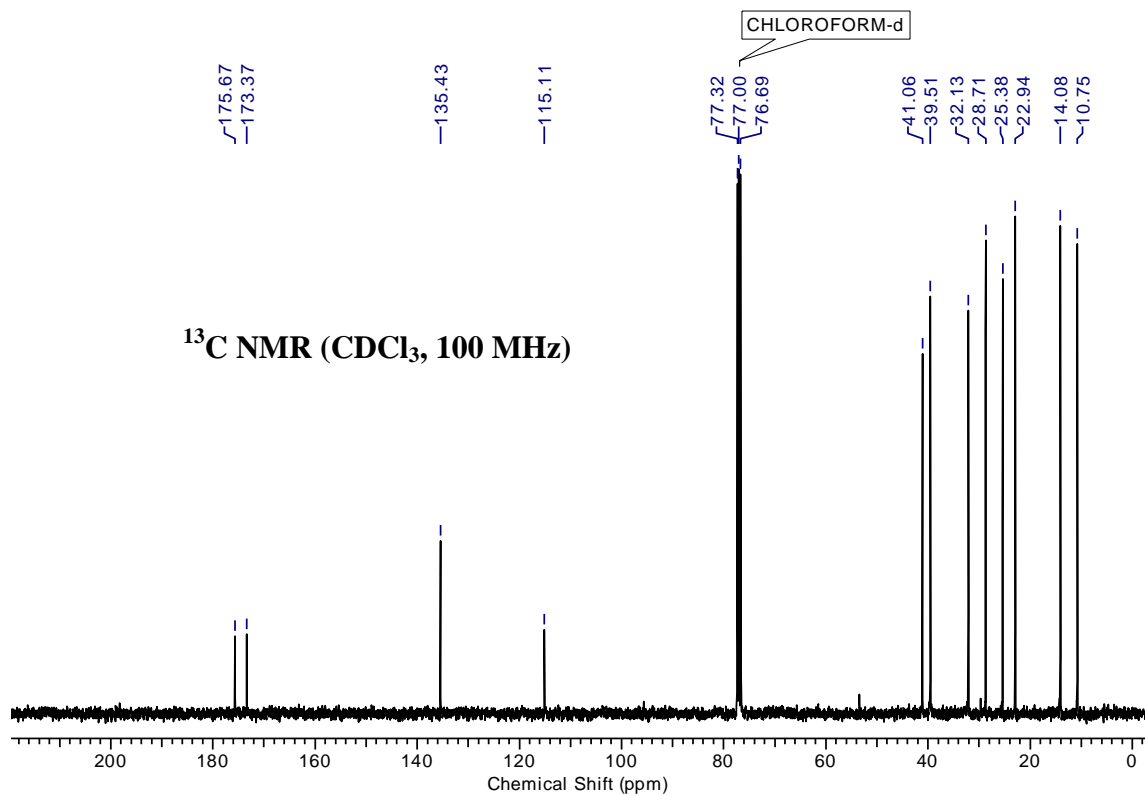


To the stirred solution of phloroglucinol (15.66 mg, 0.12 mmol) and **1a** (236.25 mg, 0.56 mmol) in anhydrous acetonitrile, triethylamine (104 μ L, 0.75 mmol) was added dropwise followed by silver nitrate (47.08 mg, 0.27 mmol). The reaction mixture was heated to 75 $^{\circ}$ C for 12 h. The reaction mixture, after being cooled to room temperature, was filtered using celite[®]. The filtrate was concentrated *in vacuo* and purified by column chromatography (eluent: 50% dichloromethane: petroleum ether, R_f = 0.5) to furnish **2a** as dark orange oil (79 mg, 51%); IR (CHCl_3) ν (cm^{-1}): 2958, 2925, 2857,

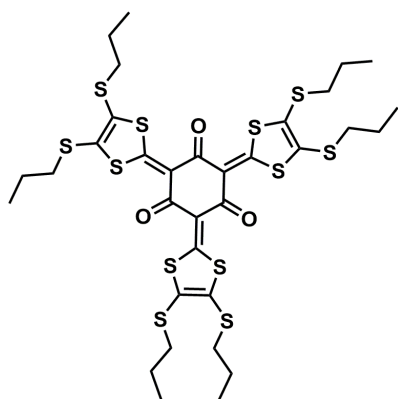
1537, 1462, 1411, 1030, 809; ^1H NMR (400 MHz, chloroform-*d*) δ = 3.12 - 3.00 (m, 12H), 1.68 - 1.55 (m, 6H), 1.55 - 1.38 (m, 24H), 1.37 - 1.21 (m, 24H), 0.91 (t, J = 7.3 Hz, 36H); ^{13}C

NMR (100 MHz, chloroform -*d*) δ = 175.7, 173.4, 135.4, 115.1, 41.1, 39.5, 32.1, 28.7, 25.4, 22.9, 14.1, 10.7; MALDI-TOF/TOF: 1291.48 (M+H)⁺, 1313.48 (M+Na)⁺, 1329.45 (M+K)⁺.



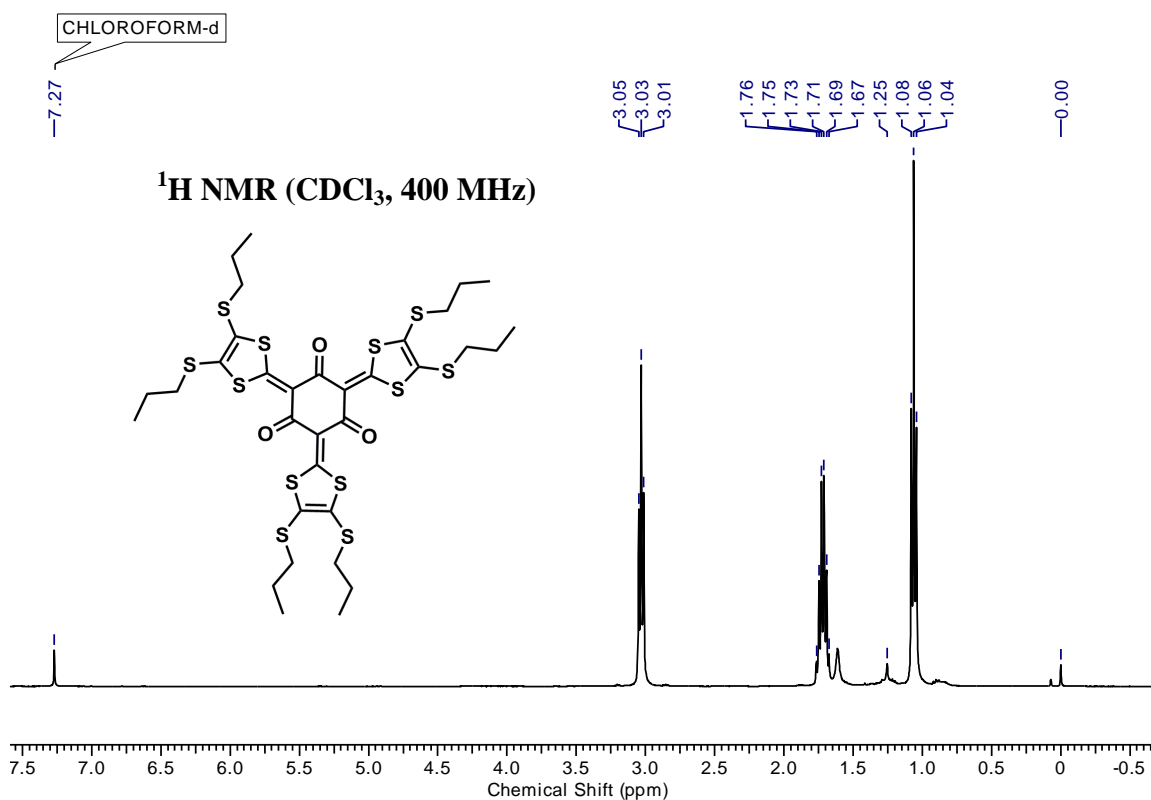


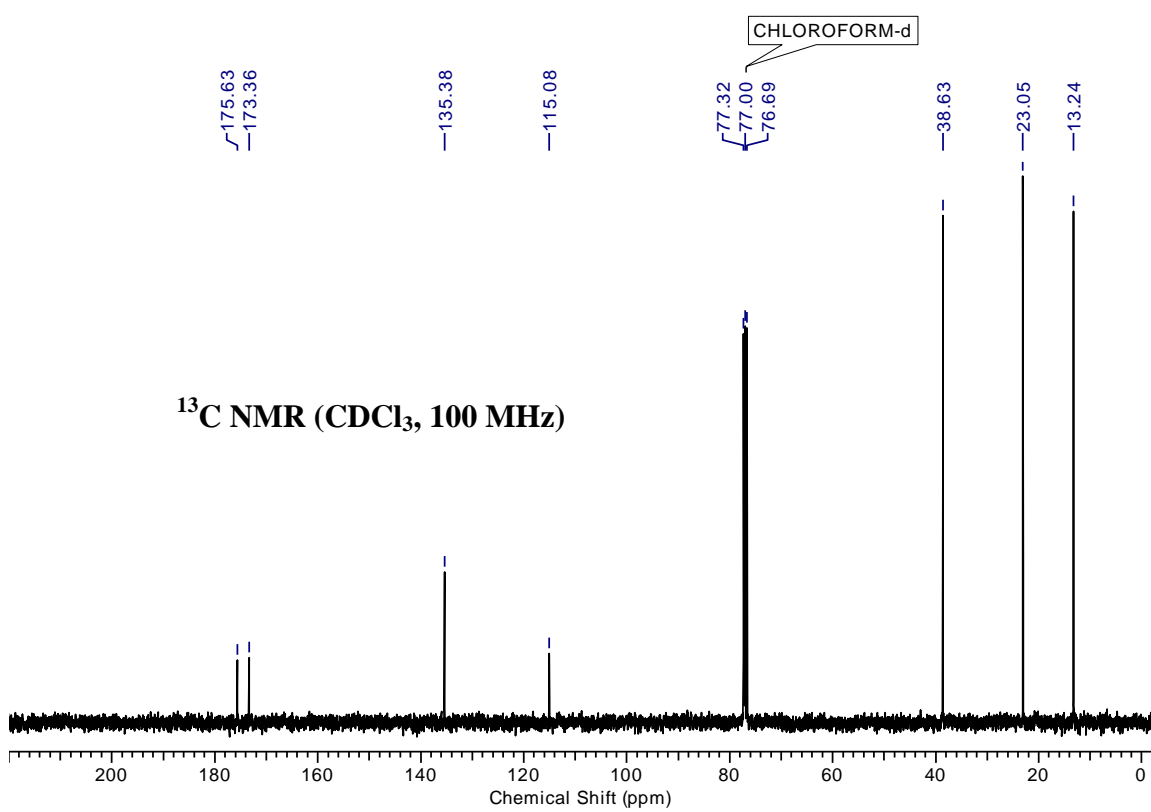
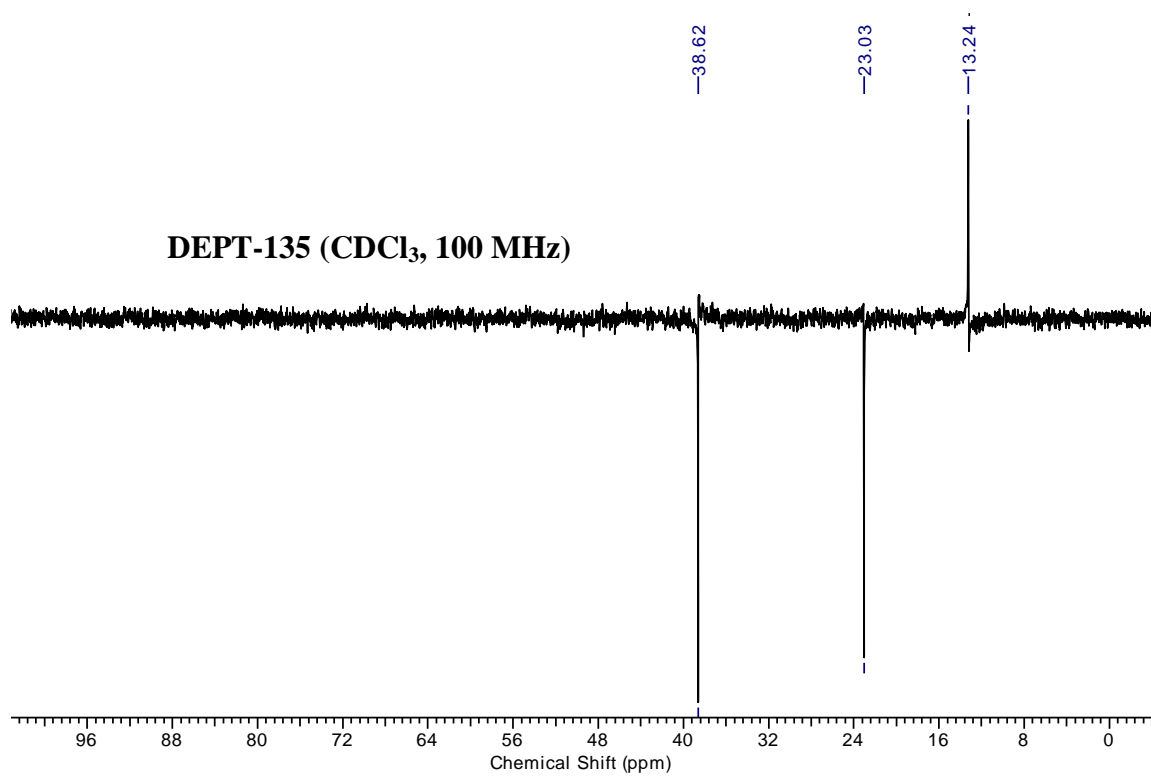
2,4,6-tris(4,5-bis(propylthio)-1,3-dithiol-2-ylidene)cyclohexane-1,3,5-trione (2b)

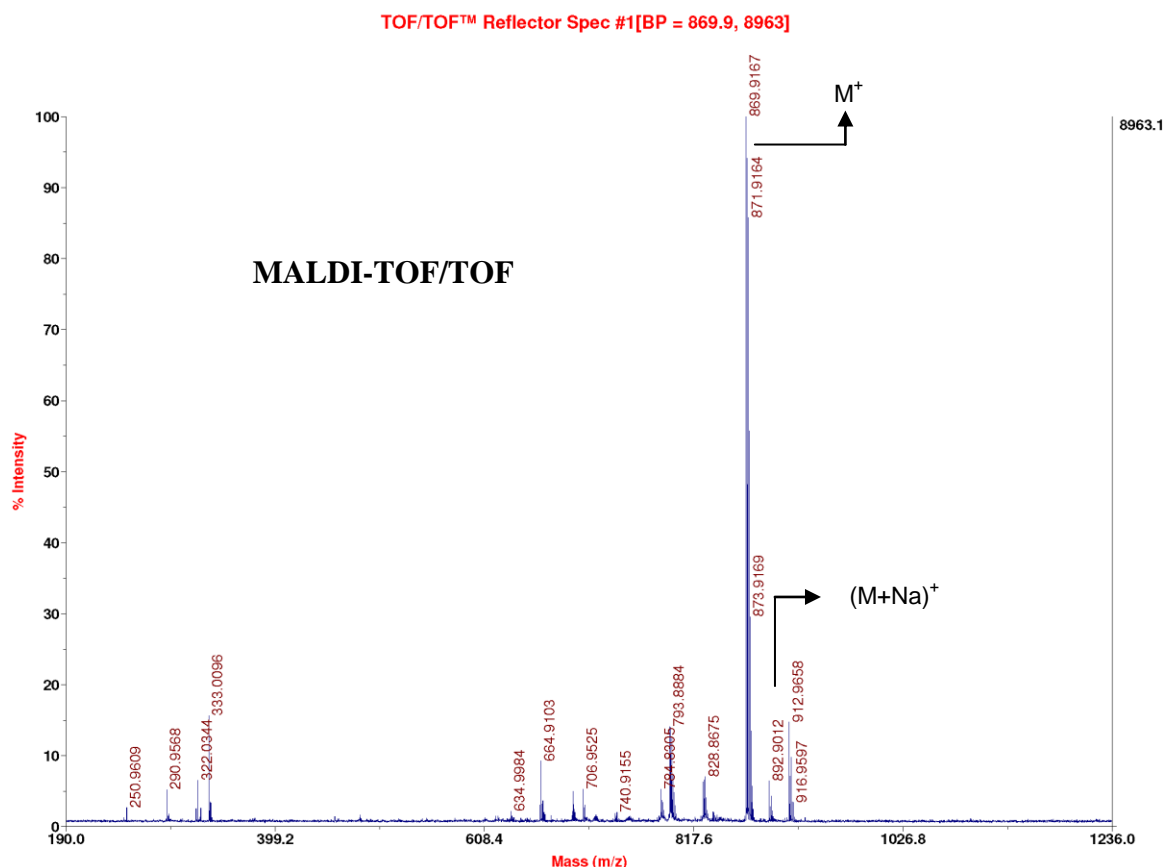


The compound **2b** was obtained following the same procedure employed for **2a** using phloroglucinol (7.8 mg, 0.06 mmol), **1b** (78.3 mg, 0.27 mmol), triethylamine (51.54 μ L, 0.37 mmol) and silver nitrate (47.08 mg, 0.27 mmol). Purification was carried out using column chromatography (eluent: 30-40% dichloromethane: petroleum ether, R_f = 0.3) to furnish **2b** as orange solid (15 mg, 28%); mp: 224-225 $^{\circ}$ C; IR (CHCl_3) ν (cm^{-1}): 1531, 1404, 1034, 928; ^1H NMR

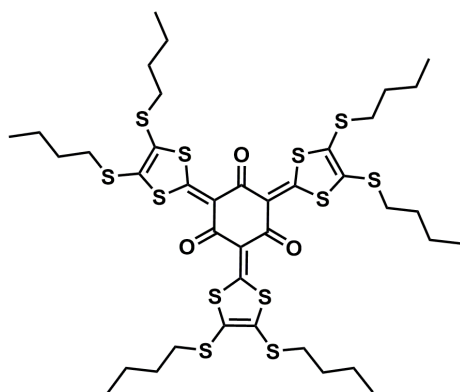
(400 MHz, chloroform -*d*) δ = 3.03 (t, J = 7.3 Hz, 12H), 1.72 (sxt, J = 7.3 Hz, 12H), 1.06 (t, J = 7.3 Hz, 18H); ^{13}C NMR (100 MHz, chloroform -*d*) δ = 175.6, 173.4, 135.4, 115.1, 38.6, 23.0, 12.2; MALDI-TOF/TOF: 869.92 (M) $^{+}$, 892.90 ($\text{M}+\text{Na}$) $^{+}$.





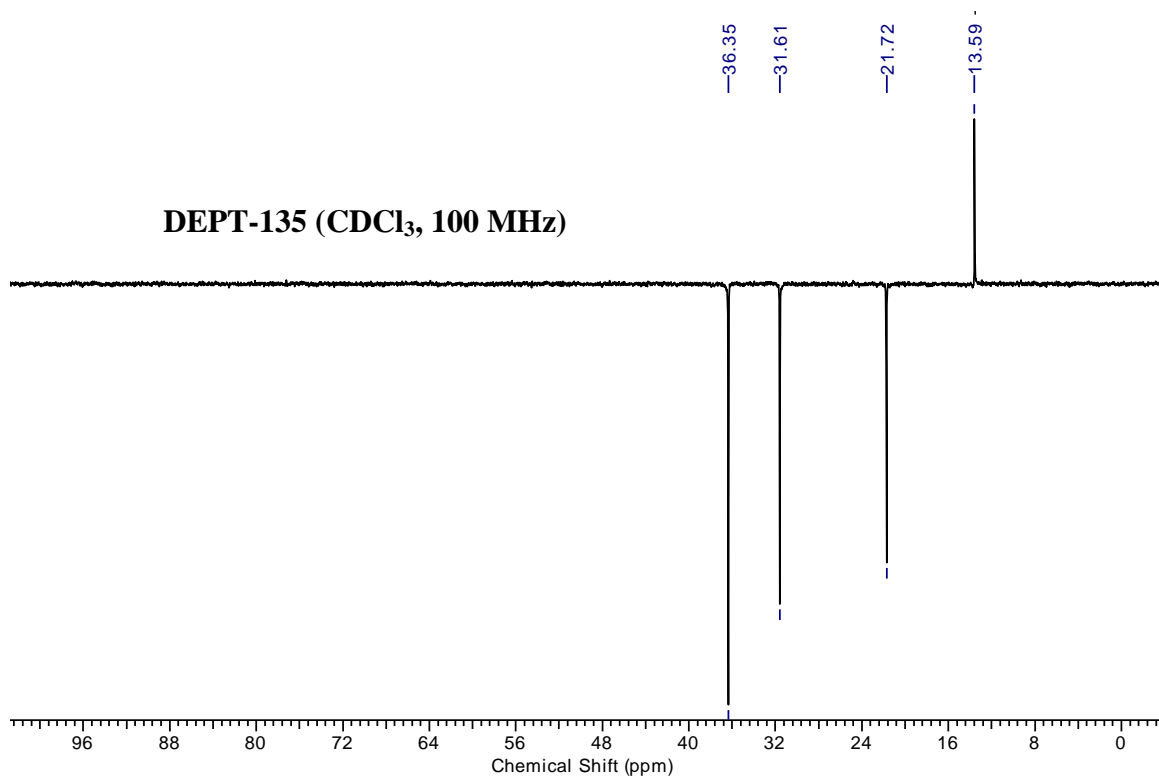
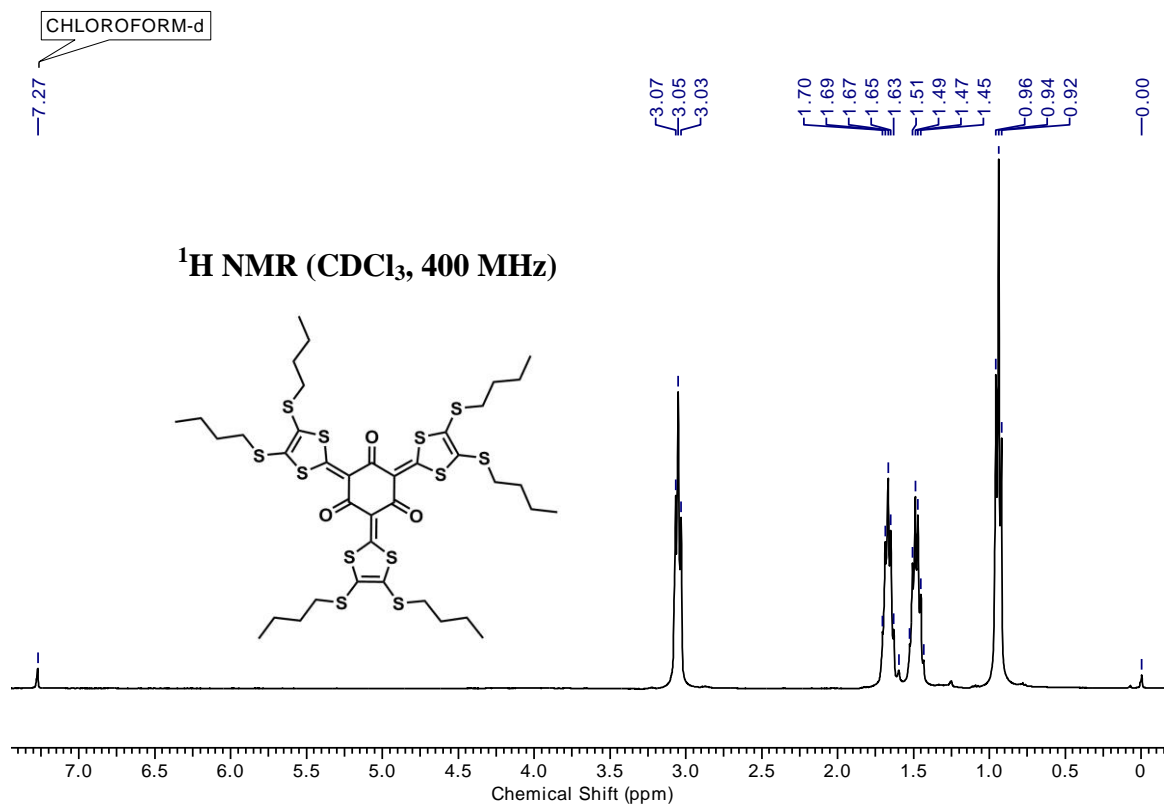


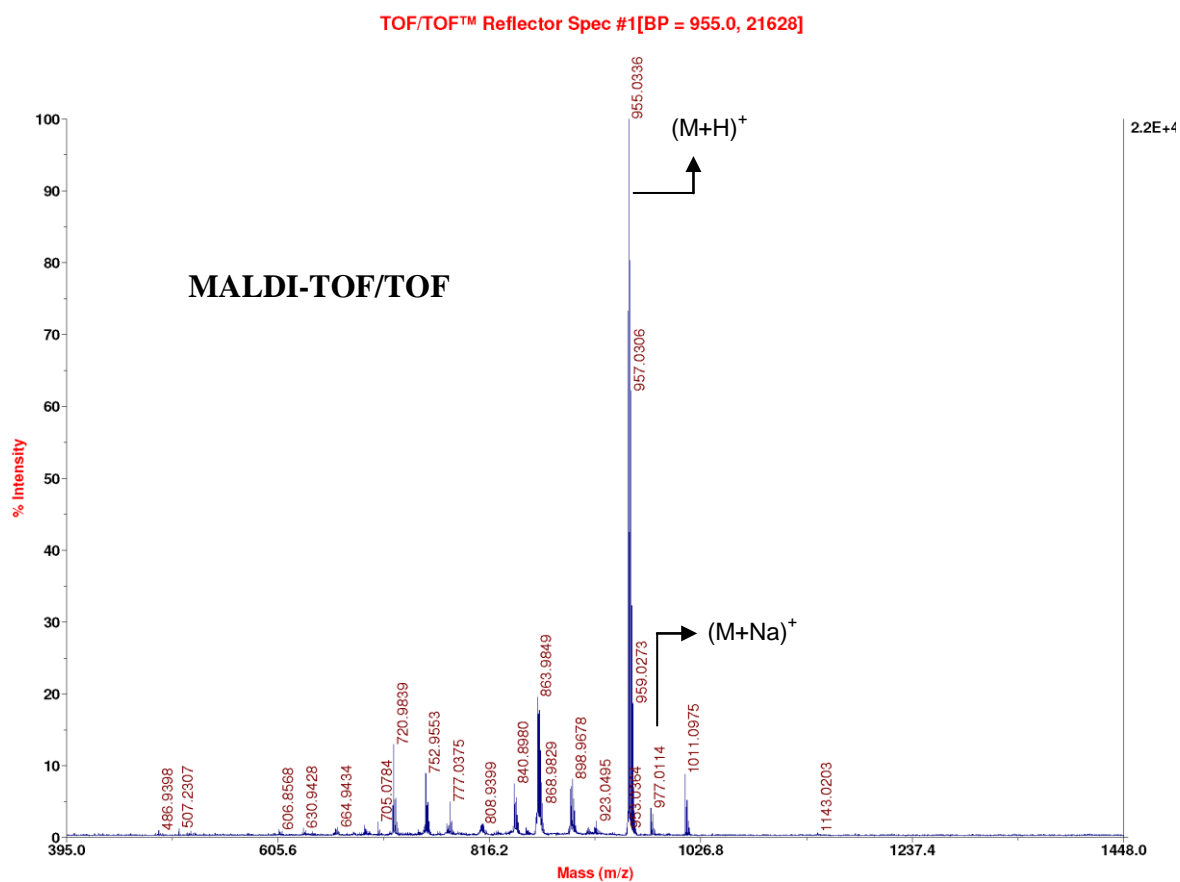
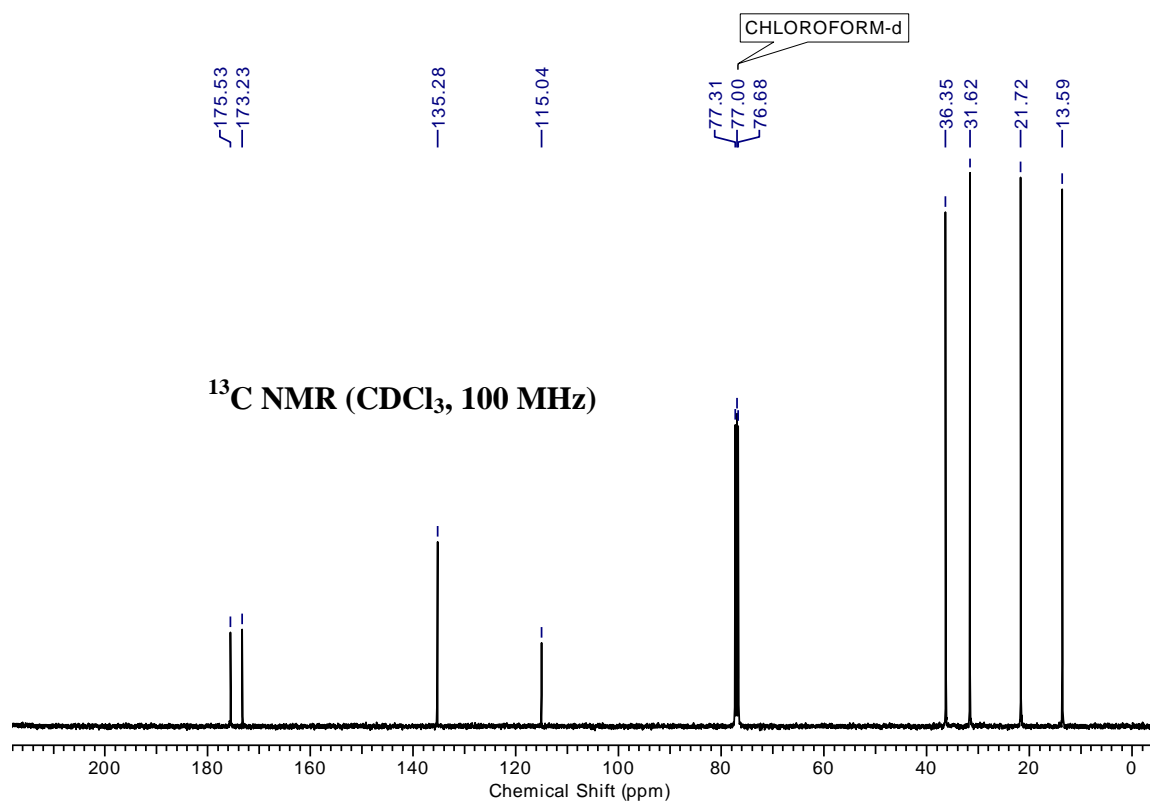
2,4,6-tris(4,5-bis(butylthio)-1,3-dithiol-2-ylidene)cyclohexane-1,3,5-trione (2c**)**



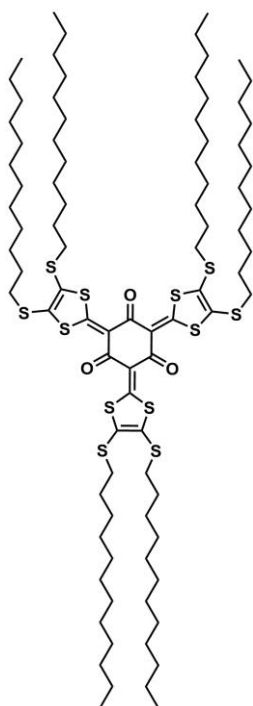
The compound **2c** was obtained following the same procedure employed for **2a** using phloroglucinol (7.61 mg, 0.06 mmol), **1c** (84.37 mg, 0.27 mmol), triethylamine (50.52 μ L, 0.36 mmol) and silver nitrate (46.14 mg, 0.27 mmol). Purification was carried out using column chromatography (30-40% dichloromethane: petroleum ether, R_f = 0.3) to furnish **2c** as orange solid (34.3 mg, 60%); mp: 145 $^{\circ}$ C; IR

(CHCl₃) ν (cm⁻¹): 1532, 1405, 1037; ¹H NMR (400MHz, chloroform-*d*) δ = 3.05 (t, J = 7.3 Hz, 12H), 1.67 (quin, J = 7.3 Hz, 12H), 1.48 (sxt, J = 7.3 Hz, 12H), 0.94 (t, J = 7.3 Hz, 18H); ¹³C NMR (100 MHz, chloroform-*d*) δ = 175.5, 173.2, 135.3, 115.0, 36.4, 31.6, 21.7, 13.6; MALDI-TOF/TOF: 955.03 (M+H)⁺, 977.01 (M+Na)⁺.

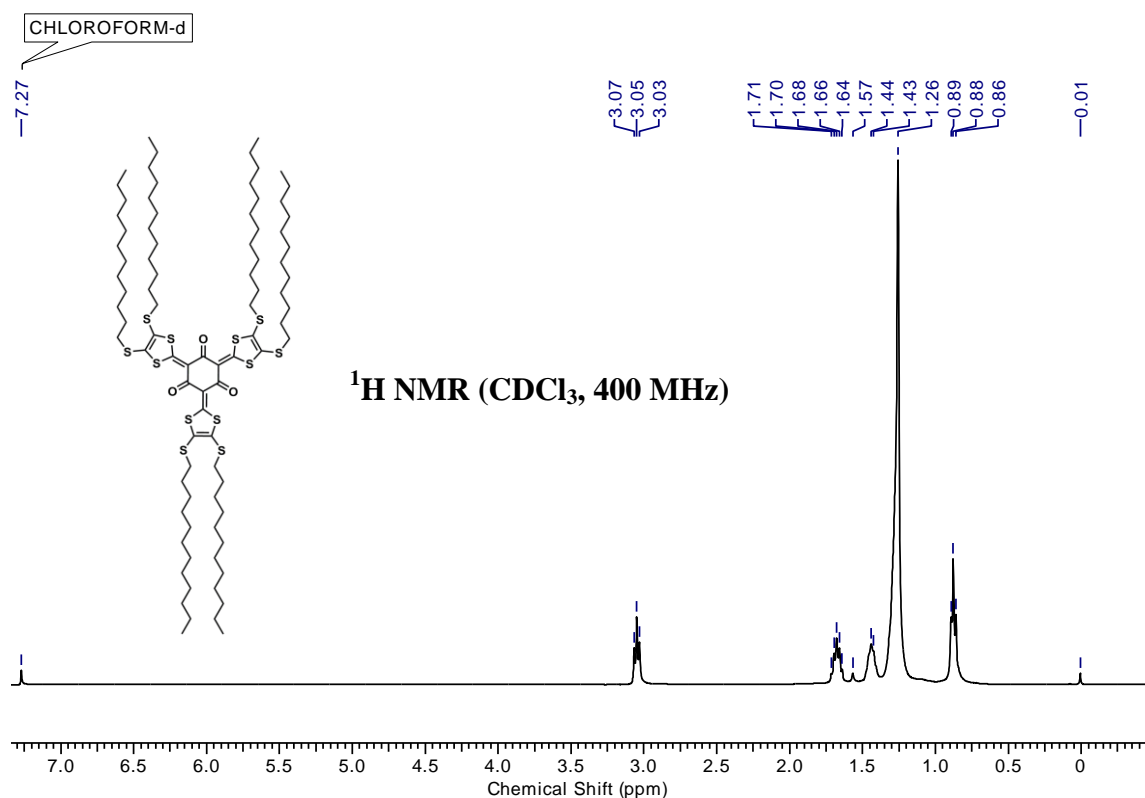


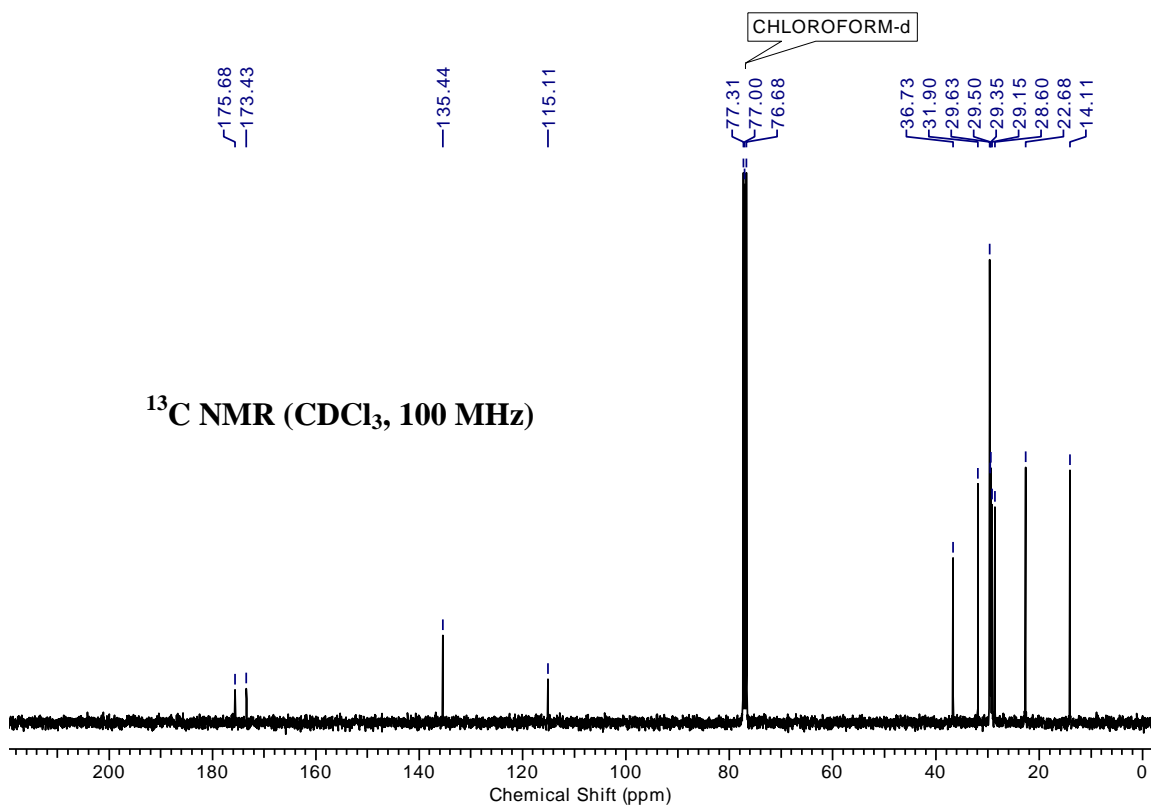
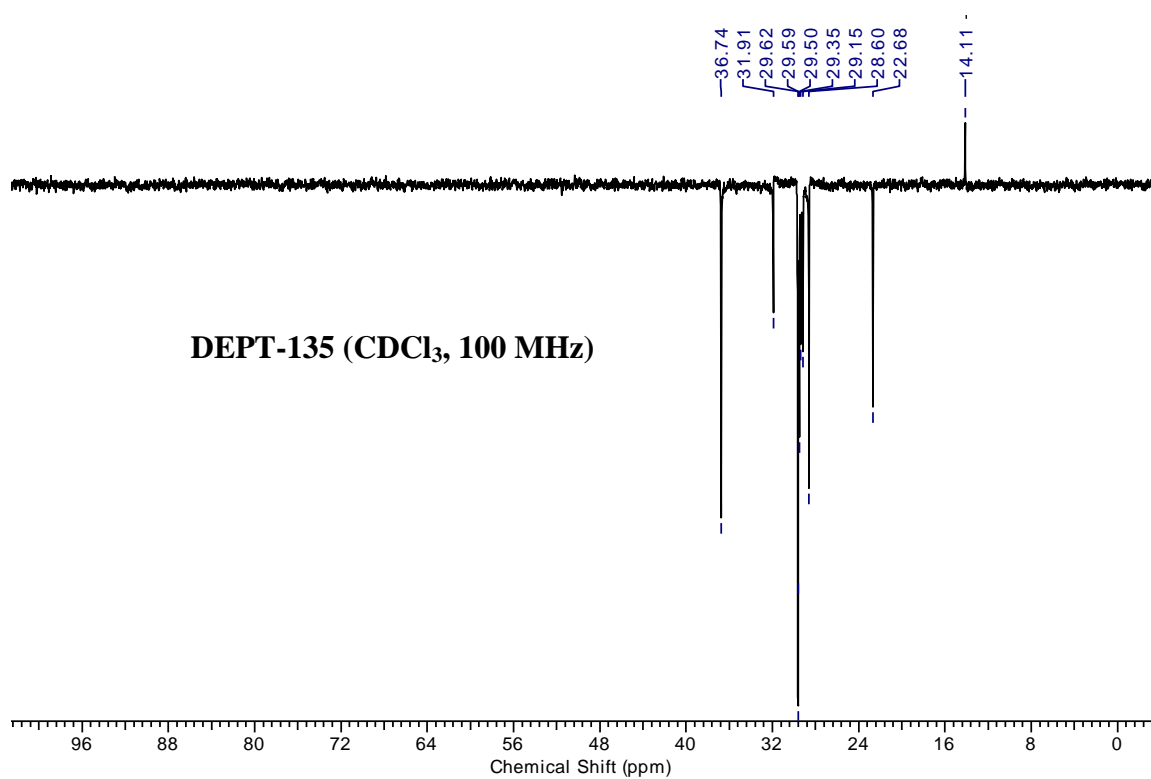


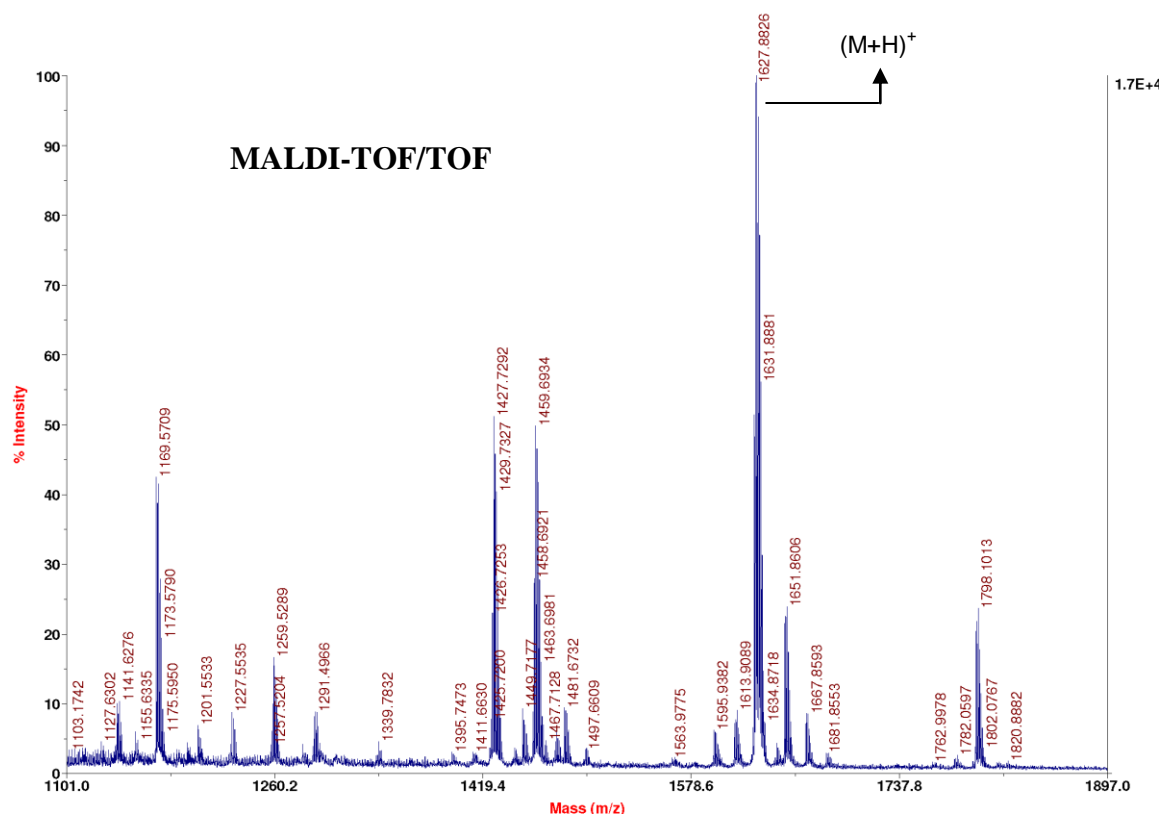
2,4,6-tris(4,5-bis(dodecylthio)-1,3-dithiol-2-ylidene)cyclohexane-1,3,5-trione (**2d**)



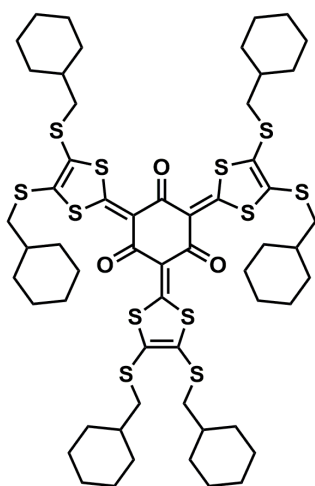
The compound **2d** was obtained following the same procedure employed for **2a** using phloroglucinol (2.98 mg, 0.02 mmol), **1d** (56.98 mg, 0.11 mmol), triethylamine (19.80 μ L, 0.14 mmol) and silver nitrate (18.06 mg, 0.11 mmol). Purification was carried out using column chromatography (20% dichloromethane: petroleum ether, $R_f = 0.3$) to furnish **2d** as orange solid (34 mg, 88%); mp: 65 $^{\circ}$ C; IR (CHCl_3) ν (cm^{-1}): 2928, 2855, 1530, 1475, 1405, 1023, 929, 850; ^1H NMR (400MHz, chloroform- d) δ = 3.05 (t, J = 7.3 Hz, 12H), 1.68 (quin, J = 7.3 Hz, 12H), 1.43 (d, J = 6.4 Hz, 12H), 1.26 (br. s., 96H), 0.88 (t, J = 6.4 Hz, 18H); ^{13}C NMR (100MHz, chloroform - d) δ = 175.7, 173.4, 135.4, 115.1, 36.7, 31.9, 29.6, 29.5, 29.4, 29.2, 28.6, 22.7, 14.1; MALDI-TOF/TOF: 1627.88 ($\text{M}+\text{H}$) $^{+}$.



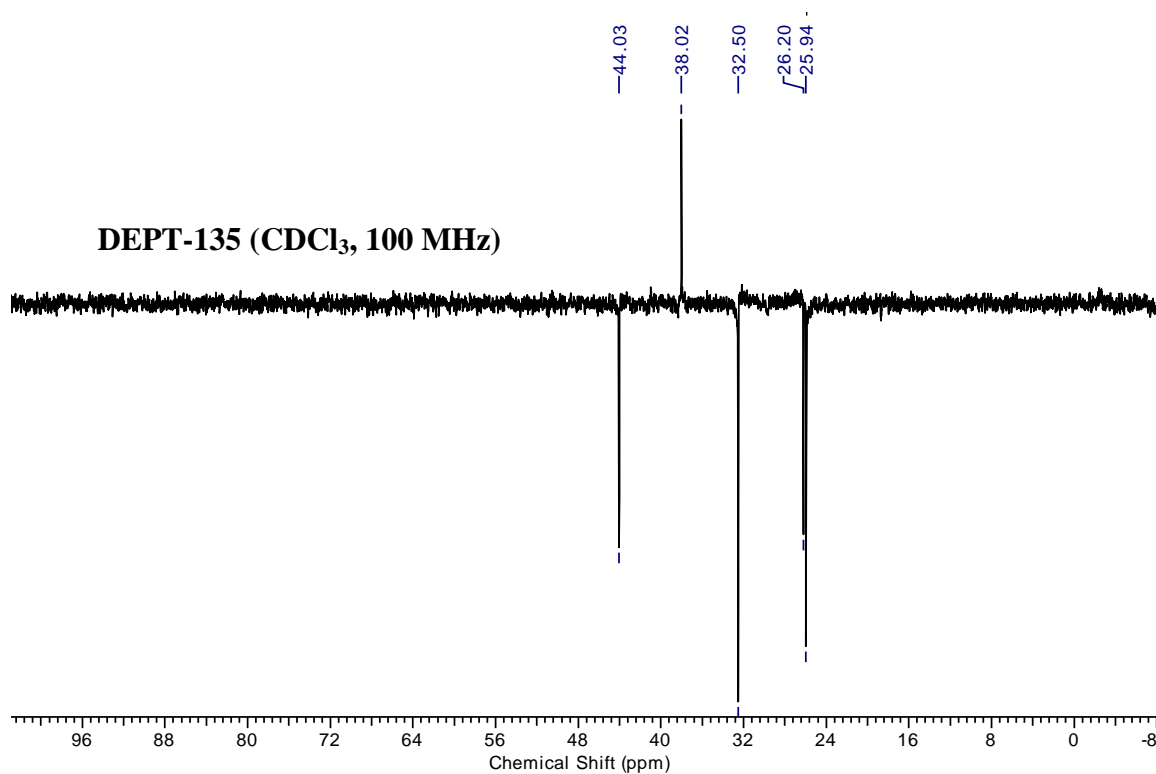
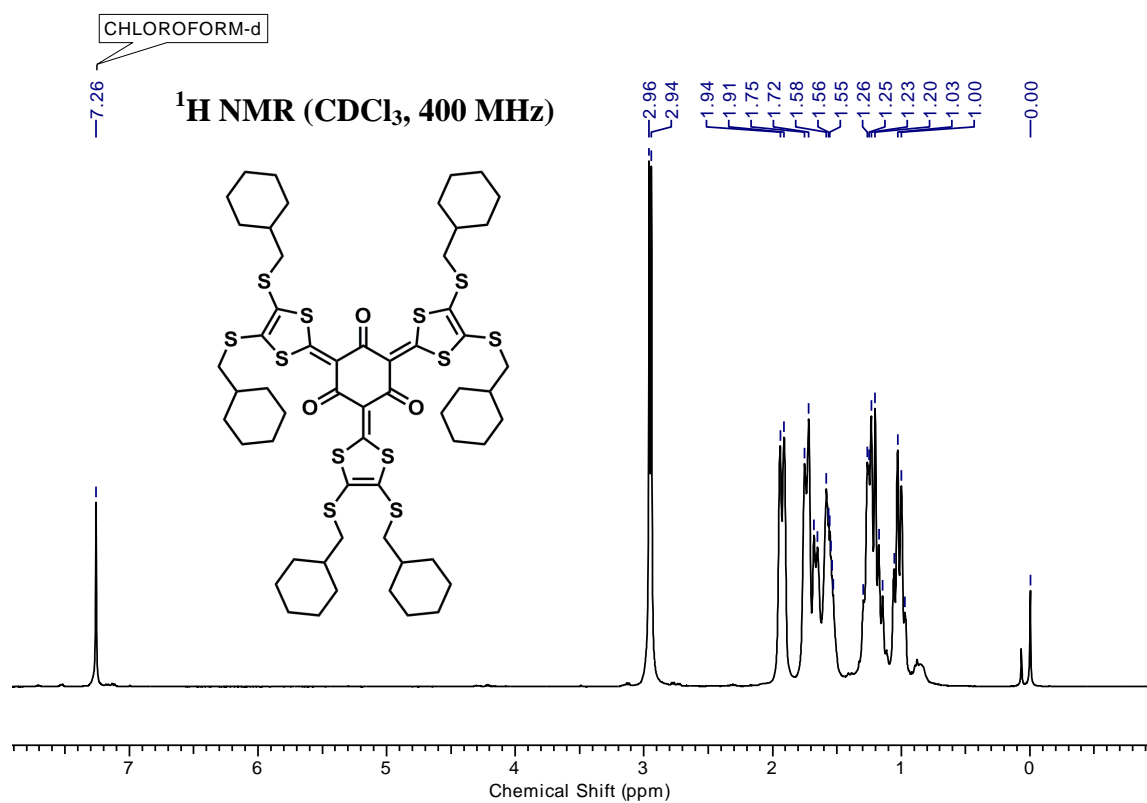


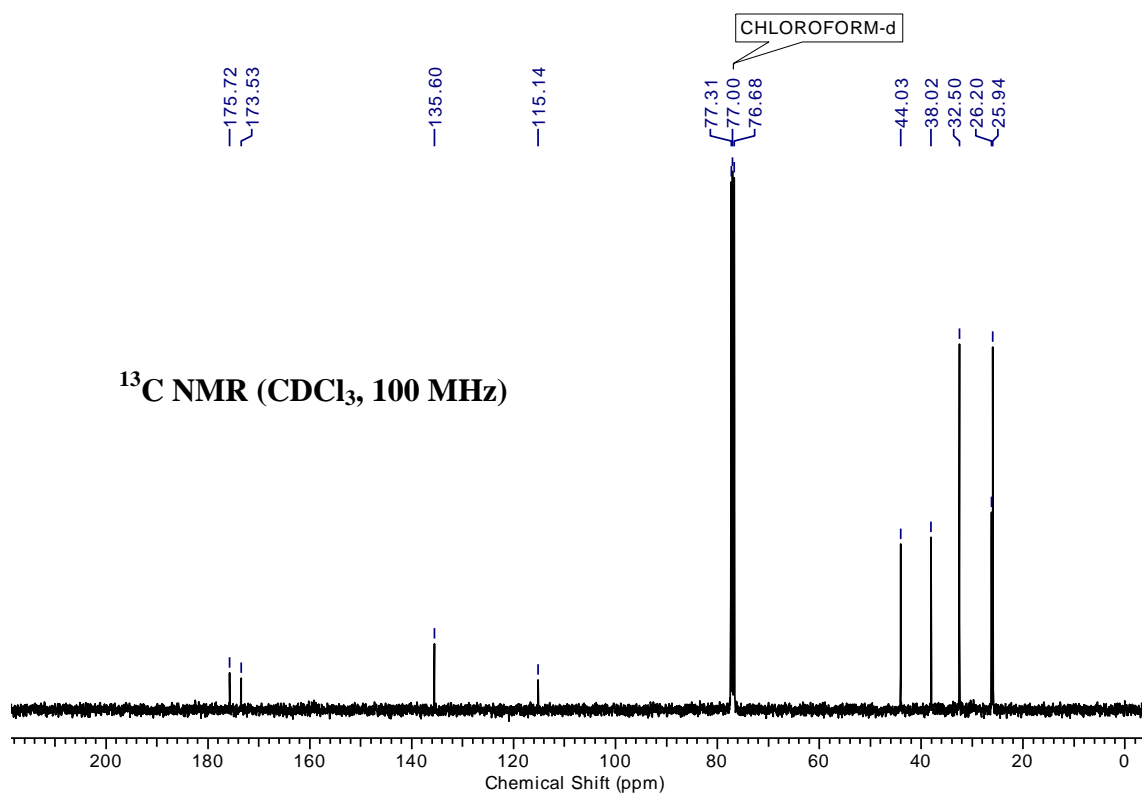


2,4,6-tris(4,5-bis((cyclohexylmethyl)thio)-1,3-dithiol-2-ylidene)cyclohexane-1,3,5-trione
(**2e**)

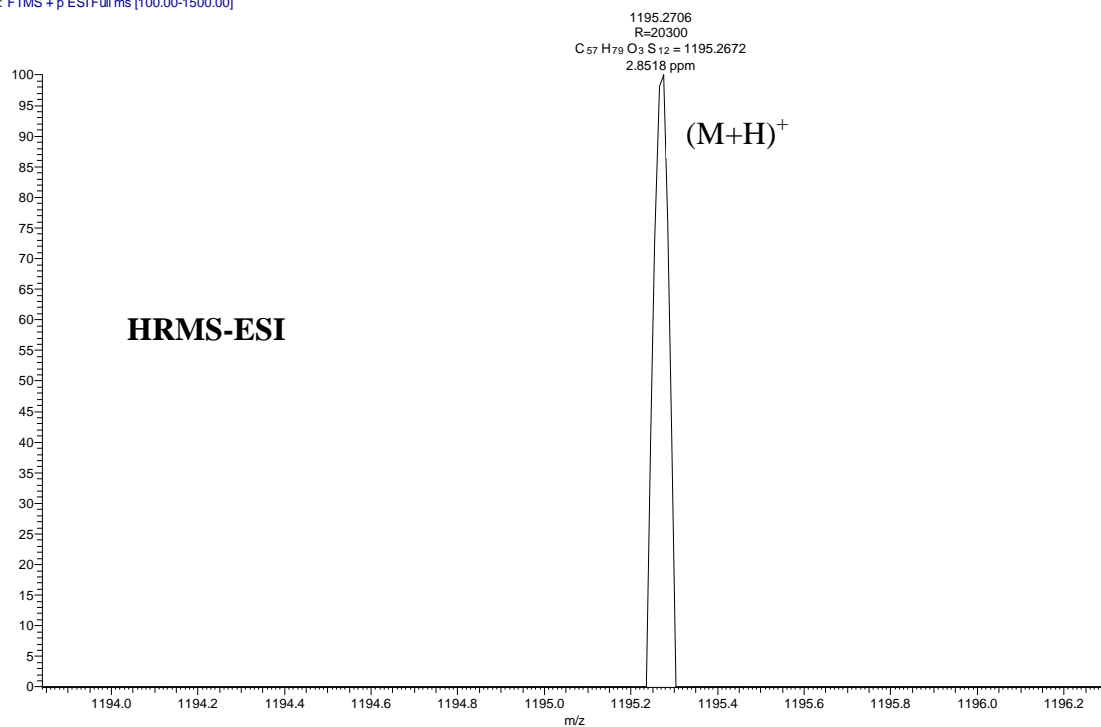


The compound **2e** was obtained following the same procedure employed for **2a** using phloroglucinol (20.95 mg, 0.17 mmol), **1e** (146 mg, 0.75 mmol), triethylamine (139 μ L, 1.00 mmol) and silver nitrate (126.99 mg, 0.75 mmol). Purification was carried out using column chromatography (2.5% ethyl acetate: petroleum ether, R_f = 0.4) to furnish **2e** as orange solid (12 mg, 6%); mp: 243-245 $^{\circ}$ C; IR (CHCl₃) ν (cm⁻¹): 1533, 1404, 1035; ¹H NMR (400 MHz, chloroform-*d*) δ = 1.92 (d, J = 11.6 Hz, 12H), 1.82 - 1.48 (m, 36H), 1.35 - 1.10 (m, 18H), 1.09 - 0.94 (m, 12H); ¹³C NMR (100 MHz, chloroform-*d*) δ = 175.7, 173.5, 135.6, 115.1, 44.0, 38.0, 32.5, 26.2, 25.9; HRMS: C₅₇H₇₉O₃S₁₂ (M+H)⁺ calcd: 1195.2672, found: 1195.2706.





CYCLO-HEX-HET-FINAL #189 RT: 0.84 AV: 1 NL: 7.26E4
T: FTMS + p ESI Full ms [100.00-1500.00]



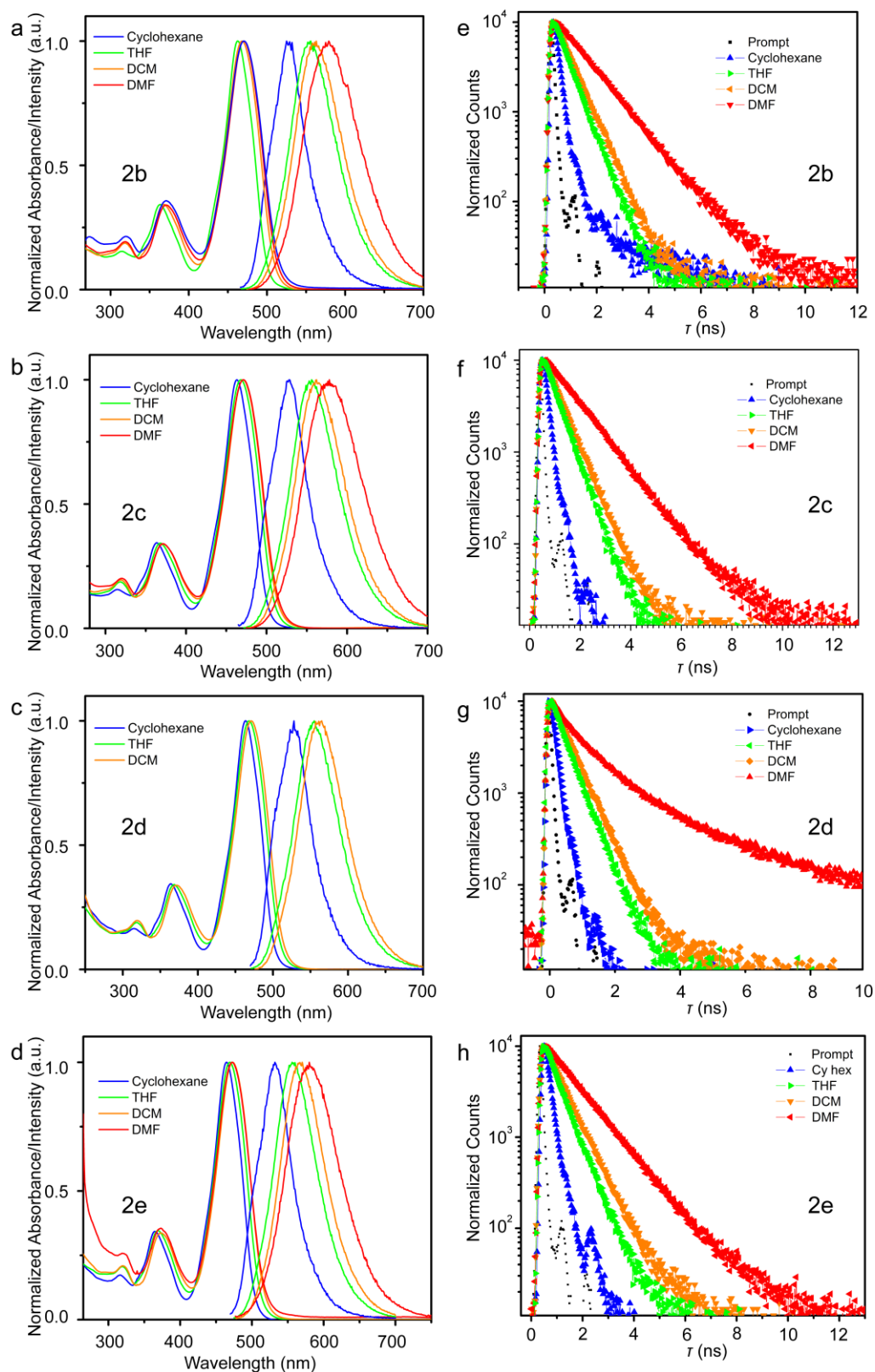


Fig. S1 Absorption and emission spectra of compounds **2b** (a), **2c** (b), **2d** (c) and **2e** (d) with their corresponding fluorescence decay **2b** (e), **2c** (f), **2d** (g) and **2e** (h) measured in various solvents at the concentration of 8 μM .

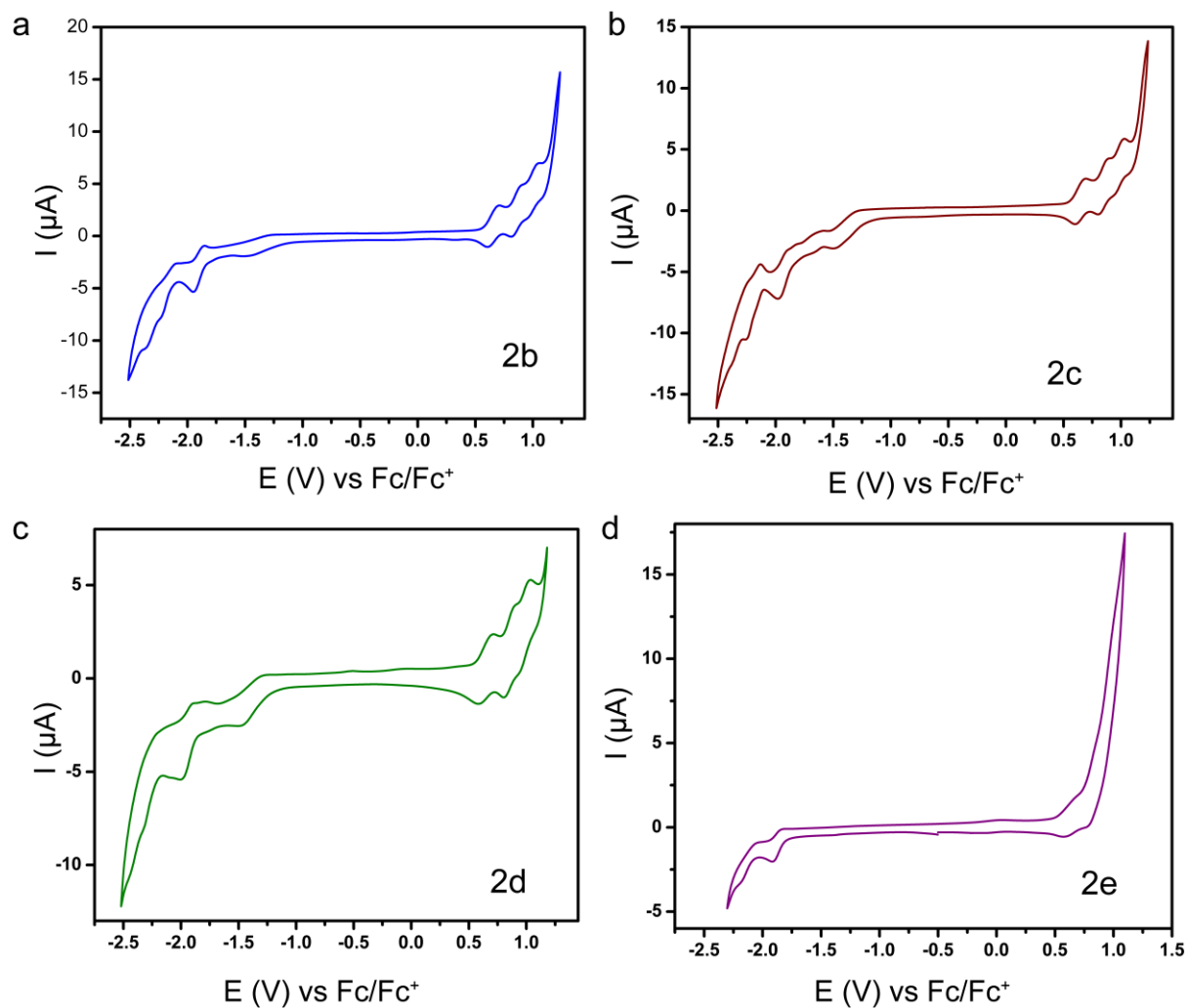


Fig. S2 Cyclic voltammetry of compound **2b-e** in dichloromethane (2×10^{-4} M) at the scan rate of 50 mVs^{-1} using Bu_4NPF_6 (0.02 M) as supporting electrolyte, glassy carbon as working, platinum wire as counter and Ag/AgCl as reference electrodes.

Table S1. Photophysical characterization of compounds **2a-e**.

Entry	λ_{\max}	λ_{em}	Stokes Shift (nm)	E_g (eV) (Optical)	τ (ns) ^a	$E_{1/2\text{ox}}$	$E_{1/2\text{red}}$	HOMO	LUMO	E_g^b (CV)
2a	472 ^a	578 ^a	106 ^a	2.40 ^b	1.140 (bi)	0.58, 0.80, 0.99	-1.96	-4.89	-2.48	2.41
2b	470 ^a	579 ^a	109 ^a	2.42 ^b	1.188 (mono)	0.65, 0.85, 1.00	-1.90	-5.09	-2.55	2.55
2c	471 ^a	578 ^a	107 ^a	2.42 ^b	1.187 (mono)	0.64, 0.84, 0.98	-1.94	-4.95	-2.55	2.40
2d	471 ^b	561 ^b	90 ^b	2.41 ^b	1.294 (tri)	0.64, 0.85, 0.99	-1.94	-5.09	-2.53	2.56
2e	473 ^a	580 ^a	107 ^a	2.40 ^b	1.193 (bi)	0.60, <i>n.d.</i> , <i>n.d.</i>	-1.87	-4.89	-2.60	2.29

Note: The superscript *a* and *b* indicate the experiments carried out in DMF and DCM, respectively; optical band gap was calculated using the formula $E_g = 1240/\lambda_{\text{onset}}$ eV; Fluorescence lifetimes were calculated using the formulae τ (biexponential) = $\tau_1 (B_1/B_1+B_2) + \tau_2 (B_2/B_1+B_2)$ and τ (triexponential) = $\tau_1 (B_1/B_1+B_2+B_3) + \tau_2 (B_2/B_1+B_2+B_3) + \tau_3 (B_3/B_1+B_2+B_3)$; $E_{1/2}$ values obtained are the mean of anodic and cathodic peak potentials vs Fc/Fc⁺; HOMO and LUMO energy levels are calculated from the onset of first oxidation and reduction waves using the formulae HOMO = $-(E_{\text{ox}} + 4.4)$ and LUMO = $-(E_{\text{red}} + 4.4)$; *n.d.* = not determined.

Table S2. Fluorescence lifetime measurements of compound **2a-e** in various solvents.

Entry	Cyclohexane	THF	DCM	DMF
2a	0.183 bi [98.2%, 1.18%]	0.522 mono	0.657 mono	1.140 bi [93.90%, 6.10%]
2b	0.160 bi [6.21%, 93.79%]	0.511 mono	0.605 mono	1.188 mono
2c	0.148 bi [98.1%, 1.9%]	0.511 mono	0.610 mono	1.187 mono
2d	0.165 bi [1.95%, 98.05%]	0.519 bi [25.74%, 74.26%]	0.630 mono	1.294 tri [8.86%, 58.14%, 33%]
2e	0.187 bi [2.35%, 97.65%]	0.546 bi [97.91%, 2.09%]	0.691 mono	1.193 bi [96.10%, 3.90%]

Note 1: Fluorescence lifetimes were calculated using the formulae τ (biexponential) = $\tau_1 (B_1/B_1+B_2) + \tau_2 (B_2/B_1+B_2)$ and τ (triexponential) = $\tau_1 (B_1/B_1+B_2+B_3) + \tau_2 (B_2/B_1+B_2+B_3) + \tau_3 (B_3/B_1+B_2+B_3)$. The percentages in the parentheses are the component contributions to the fluorescence decay. *Note 2:* The triexponential fluorescence decay observed in **2c** could be ascribed to reduced solubility in DMF.

Single crystal X-ray diffraction

X-ray intensity data measurement of compound **2e** was carried out on a Bruker D8 VENTURE Kappa Duo PHOTON II CPAD diffractometer equipped with Incoatech multilayer mirrors optics. The intensity measurements were carried out with Cu micro-focus sealed tube diffraction source ($\text{MoK}_\alpha = 0.71073 \text{ \AA}$) at 100(2) K temperature. The X-ray generator was operated at 50 kV and 1.4 mA. A preliminary set of cell constants and an orientation matrix were calculated from three sets of 36 frames. Data were collected with ω scan width of 0.5° at different settings of φ and 2θ with a frame time of 10 secs keeping the sample-to-detector distance fixed at 5.00 cm. The X-ray data collection was monitored by APEX3 program (Bruker, 2016). All the data were corrected for Lorentzian, polarization and absorption effects using SAINT and SADABS programs (Bruker, 2016). SHELX-97 was used for structure solution and full matrix least-squares refinement on F^2 . All the hydrogen atoms were placed in a geometrically idealized position and constrained to ride on its parent atom.

Table S3. Crystal data and structure refinement of compound **2e**.

Identification code	LCCYHEX_0m
Crystal Color and shape	Orange, needle
Empirical formula	$\text{C}_{57}\text{H}_{78}\text{O}_3\text{S}_{12}$, CHCl_3
Formula weight	1315.28
Temperature/K	100(2)
Crystal system and space group	Triclinic, $P-1$
$a/\text{\AA}$	9.9099(6)
$b/\text{\AA}$	17.0949(11)
$c/\text{\AA}$	19.8240(13)
$\alpha/^\circ$	111.1910(10)
$\beta/^\circ$	99.8140(10)
$\gamma/^\circ$	94.4630(11)
Volume/ \AA^3	3049.7(3)
Z	2
$\rho_{\text{calc}} (\text{g/cm}^3)$	1.432
μ/mm^{-1}	0.605

F(000)	1388.0
Crystal size/mm ³	0.4 x 0.14 x 0.14
Radiation	MoK α λ =0.71073 Å
2 Θ max/°	50.000
Index ranges	-11 \leq h \leq 11, -20 \leq k \leq 20, -23 \leq l \leq 23
Independent reflections	9623
Completeness to theta=25.000	100%
Goodness-of-fit on F ²	1.015
Final R indexes [$I \geq 2\sigma(I)$]	R ₁ = 0.0297, wR ₂ = 0.0685

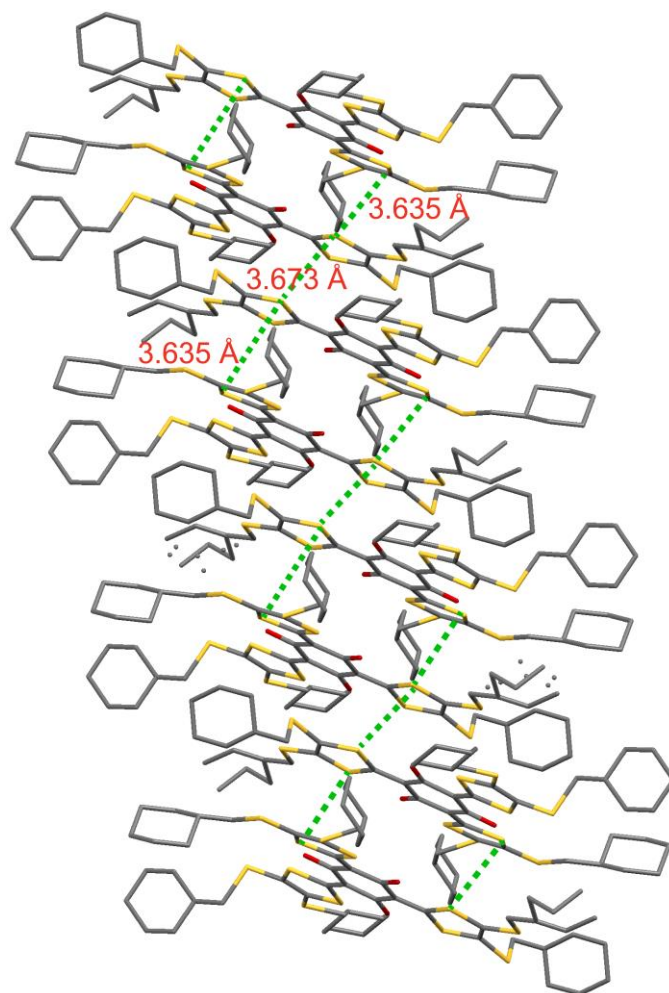


Fig. S3 Crystal packing approximately along the *b* axis. The green dotted lines indicate the intermolecular S...S contacts.

Self-Assembly

Compound 2b

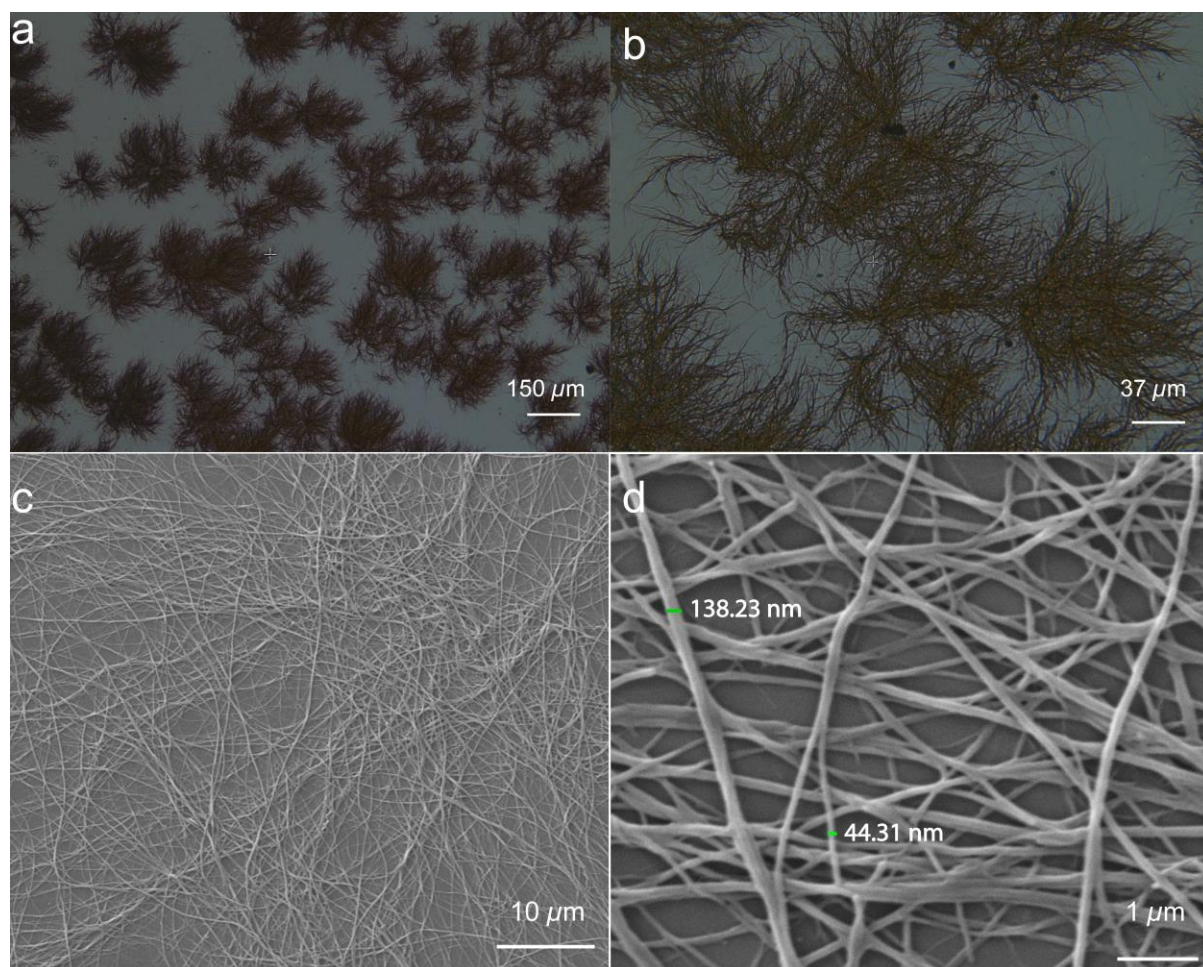


Fig. S4. Representative optical (a, b) and scanning electron (c, d) microscopy images of **2b** (1 mM, 10 μL) drop-casted on a silicon substrate using DMF as solvent.

Compound 2c

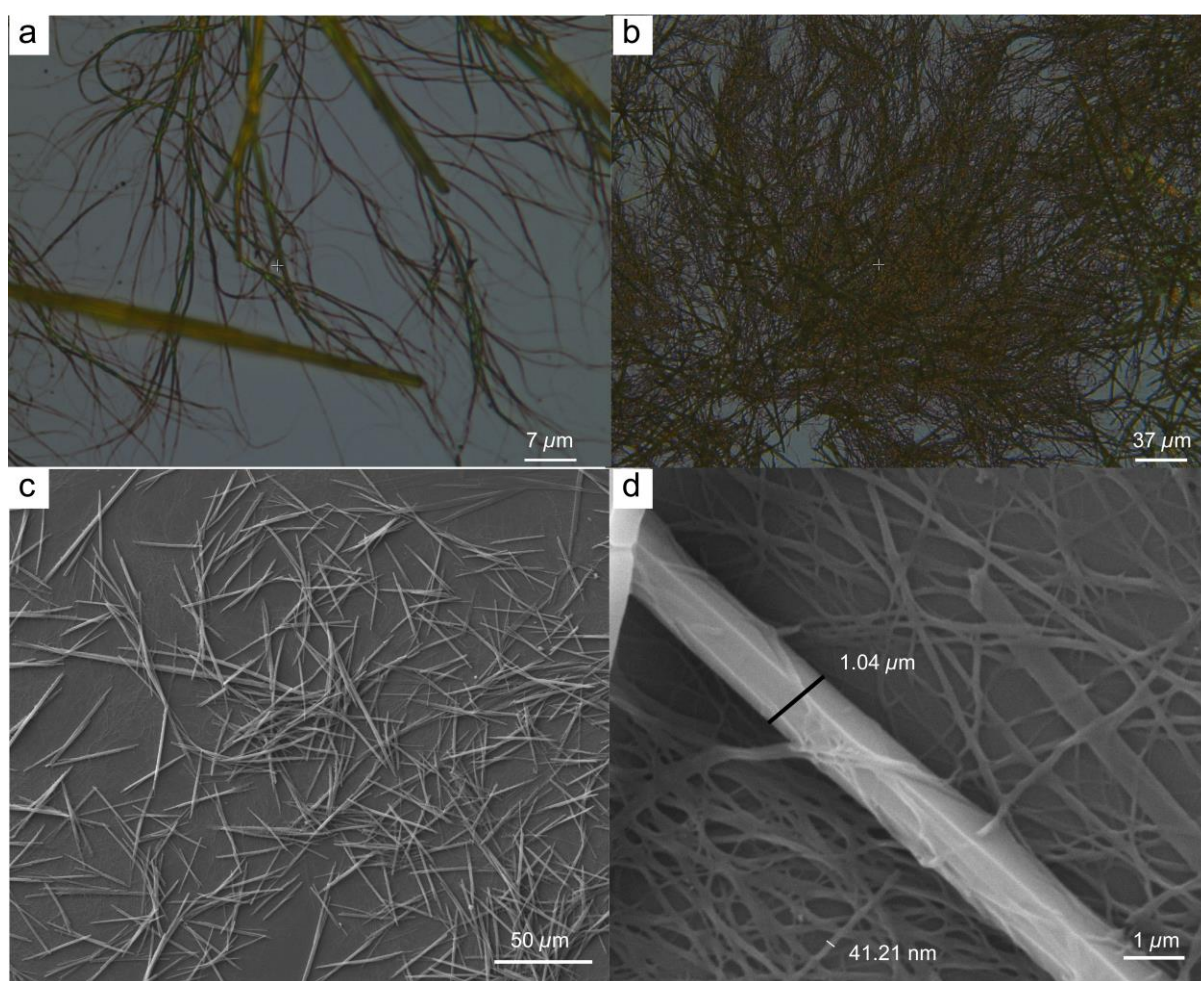


Fig. S5 Representative microscopy images of compound **2c** obtained by drop-casting 1mM DMF solution (10 μ L) on a silicon substrate using DMF as solvent. Optical microscopy (a,b) and SEM images (c,d).

AFM section analysis of 2b nanofibres

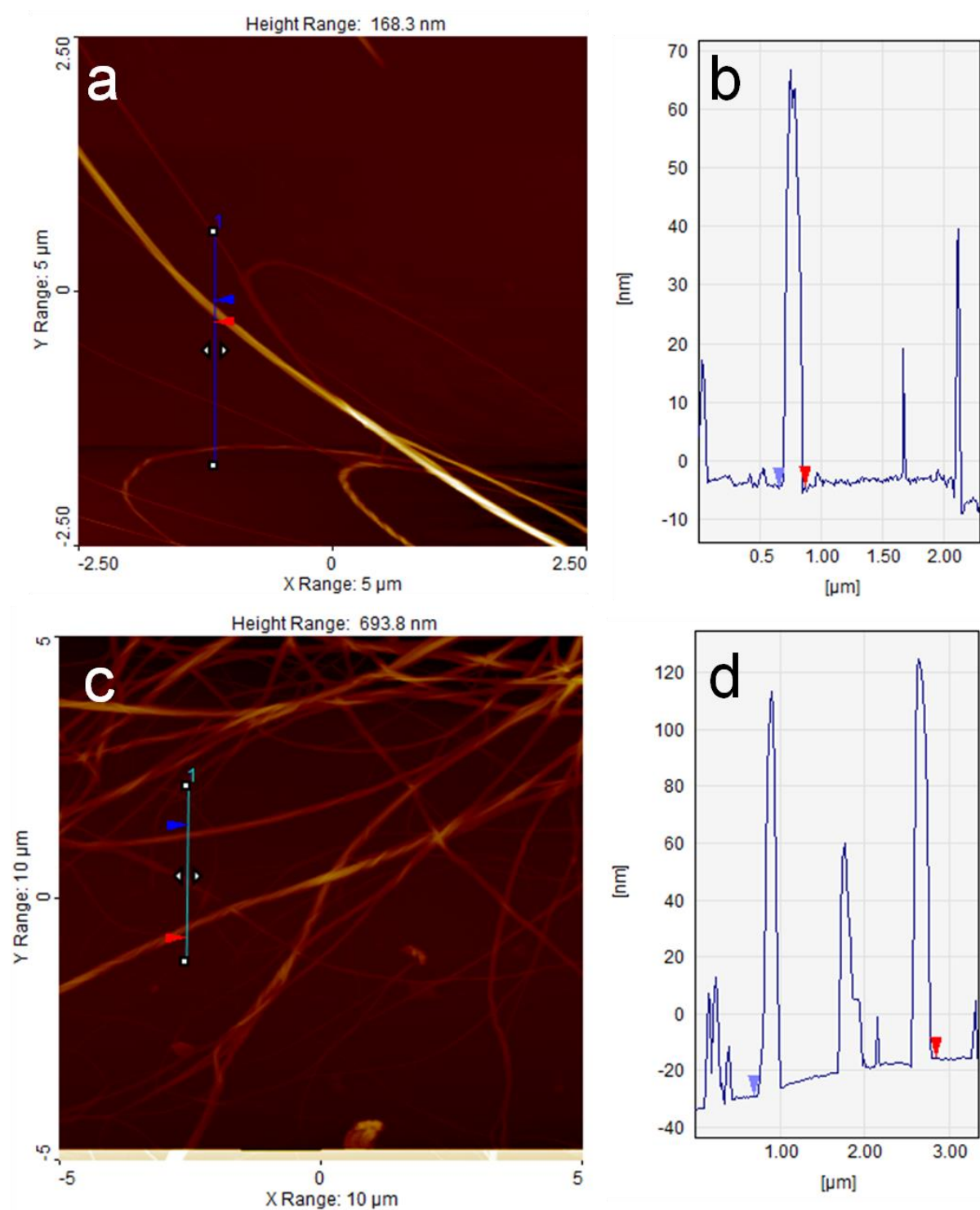


Fig. S6 AFM images of nanofibres obtained by drop-casting 0.1 mM DMF solution (10 μL) of **2b** (a, c) on a monocrystalline silicon wafer and their corresponding section analysis (c, d).

Compounds 2a, 2d and 2e

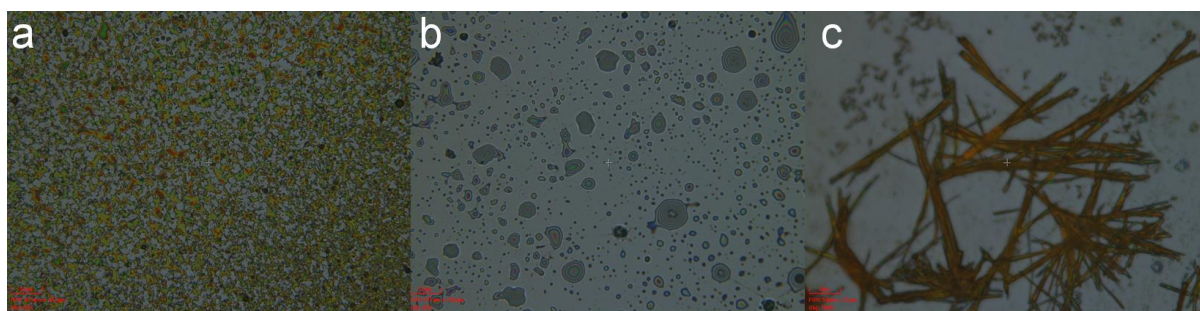


Fig. S7 Representative optical microscopy images of compounds **2a** (a), **2d** (b) and **2e** (c) obtained by drop-casting their 1 mM DMF solution (10 μ L) on silicon substrates showing no discernible supramolecular structures in **2a** and **2d**, and microcrystals in **2e**.

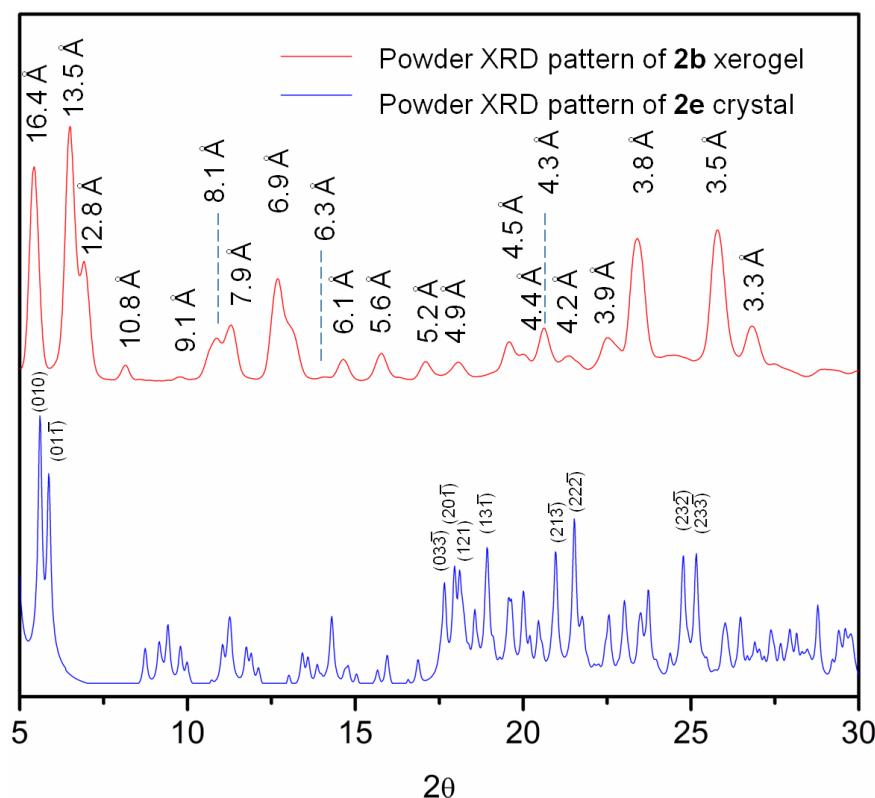


Fig. S8 Powder XRD profiles of **2b** xerogel and **2e** crystal obtained from DMF, and 3:1 (v/v) mixture of chloroform and methanol, respectively. The corresponding d spacing distances and Miller indices are assigned above the peaks observed in **2b** xerogel and for major reflexes in **2e** crystal, respectively.

The crystalline **2e** showed pointed reflexes in the powder XRD pattern (Fig. S8) with the peak having highest intensity observed at 5.6° (2θ), corresponding to the b plane possessing Miller index (010) and d spacing distance of 15.7° . This distance is in agreement with the length of the repeating stack of **2e** molecules (Fig. S9a). Similar to **2e**, self-assembled **2b** nanofibres exhibit sharp reflexes from low to wide angles in the PXRD pattern and point to its crystalline behaviour (Fig. S8). We estimated the end-to-end length of the **2b** molecule from the energy minimized structure obtained by molecular mechanics (MM2) method in Chem3D Pro version 13.0.2.3021 and found it to be 17.2 \AA (Fig. S9b). Indexation of the observed PXRD peaks employing *LCDiXRay* program² unveiled columnar array of **2b** with a parallelogram lattice, widely termed as columnar oblique (Col_{ob}) ($p1$ symmetry) arrangement (Fig. S9c). While the liquid crystalline compounds possess sharp low angle reflexes accompanied with diffused wide angle reflection,³ the crystalline **2b** displays several spikes in the wide angle region, signifying that the alkyl chains are not segregated from the main core. The parallelogram lattice with parameters $a = 26.2 \text{ \AA}$, $b = 32.9 \text{ \AA}$ and angle between the axes $\gamma = 55.2^\circ$ possesses lattice area (S) and unit cell volume (V) of 705.22 \AA^2

and 2327.6 \AA^3 , respectively. The number of molecules present in unit cell (Z) was found to be 1.6 (Table S4). Furthermore, the d spacing distances of $3.8\text{-}3.3 \text{ \AA}$ could be attributed to the intermolecular $\text{S}\cdots\text{S}$ and π -stacking interactions in the **2b** J -aggregate nanofibre.

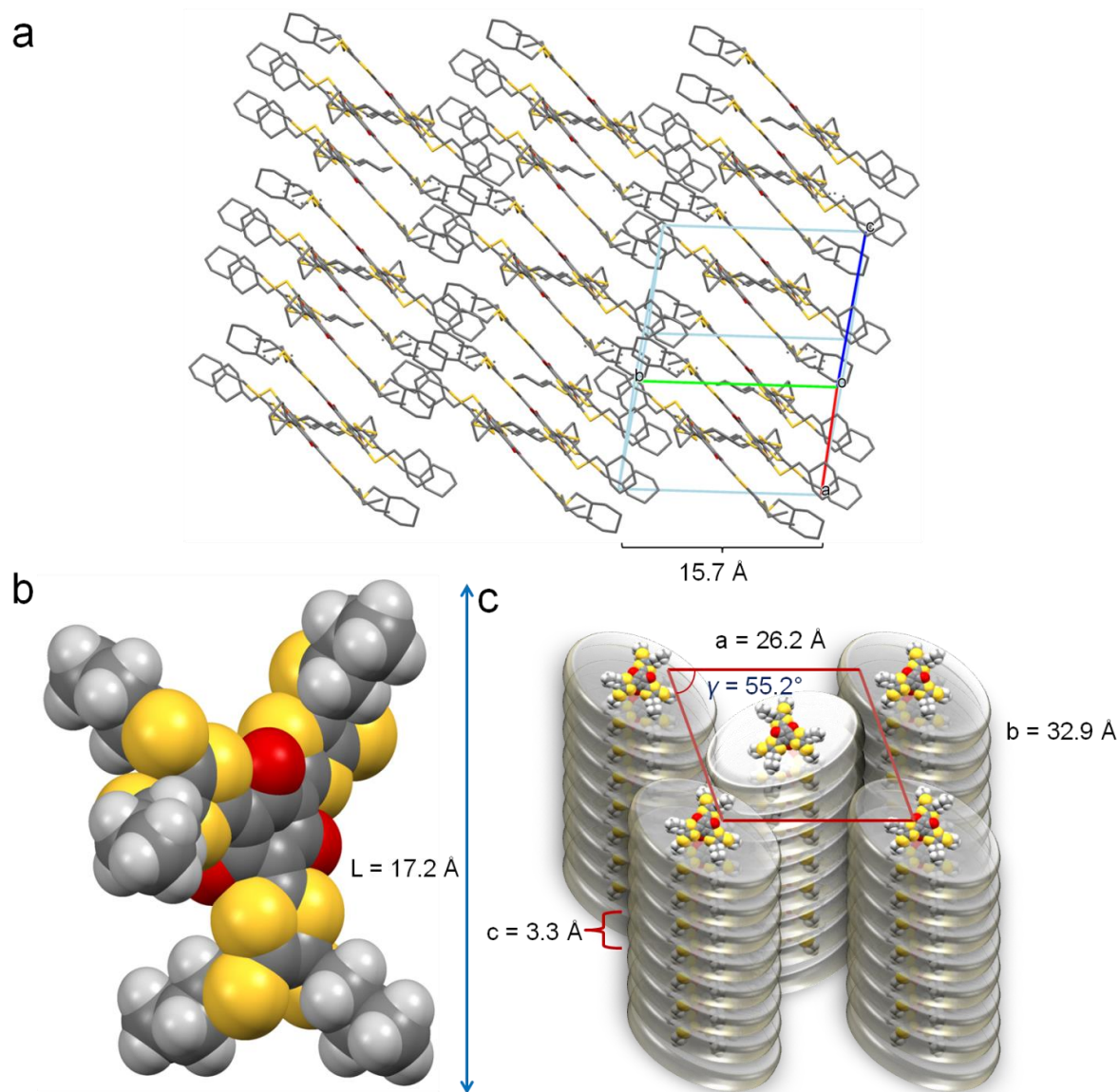


Fig. S9 (a) Crystal packing observed in **2e** showing a representative unit cell with (010) or b plane possessing d spacing distance (15.7 \AA) approximately in agreement with the length of the molecule. (b) Energy minimized structure of **2b** with length corresponding to 17.2 \AA . (c) Schematic showcasing the self-assembly of **2b** xerogel into columnar oblique (Col_{ob}) arrangement.

Table S4 Indexation results obtained for the XRD profile of **2b** xerogel at room temperature

Phase Symmetry	$d_{\text{obs}}(\text{\AA})$	$d_{\text{cal}}(\text{\AA})$	Miller indices hk	Lattice parameters (\AA), lattice area S (\AA^2), molecular volume V (\AA^3)
Col _{ob} $p1$	16.40	16.40	12	$a = 26.16$
	13.50	13.50	02	$b = 32.88$
	12.80	12.80	21	$\gamma = 55.20^\circ$
	10.80	10.78	13	$S = 705.22$
	9.10	9.00	03	$V = 2327.6$
	8.10	8.17	31	$Z = 1.61$
	7.90	7.85	14	
	6.90	7.00	-13	
	6.30	6.31	44	
	6.10	6.11	-31	
	5.60	5.59	-14	
	5.20	5.20	53	
	4.90	5.00	52	
	4.50	4.50	06	
	4.40	4.35	64	
	4.30	4.30	50	
	4.20	4.21	66	
	3.90	3.91	-51	
	3.80	3.76	-43	
	3.50	3.50	-26	
	3.3	----		

The lattice area (S), lattice volume (V) and number of molecules per unit cell (Z) were calculated using the formulae: $S = ab\sin\gamma$; $V = S \times c$; $Z = \rho N_A V / M$, where ρ is density considered as 1, N_A is the Avogadro's number, V is the molecular volume, and M is the molecular weight of **2b**, which is 871.42.

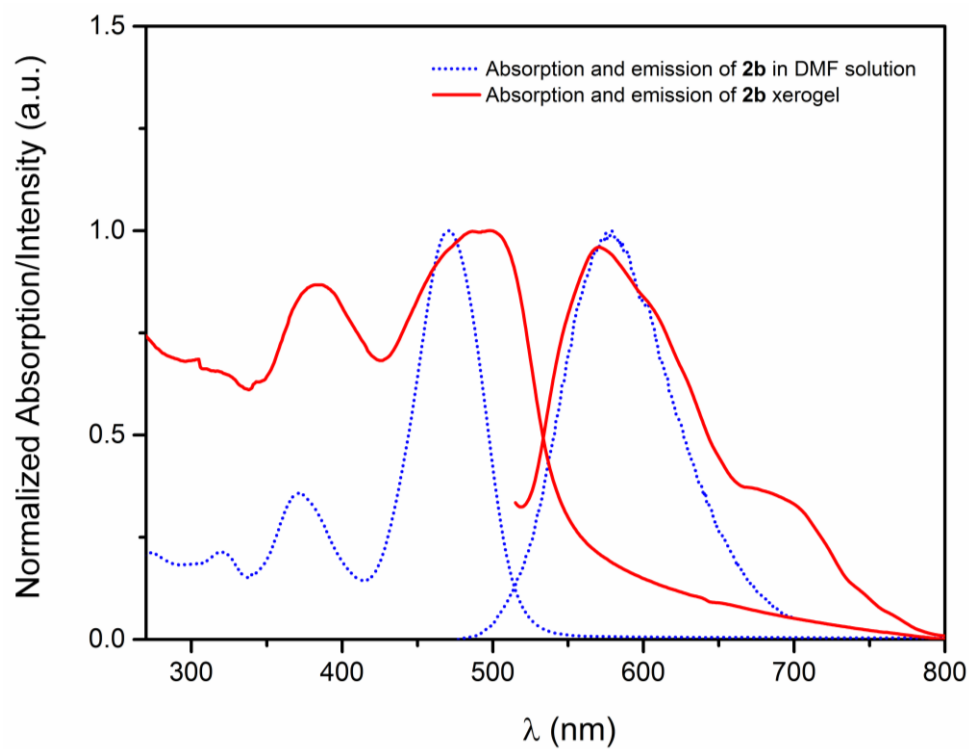


Fig. S10 Absorption and emission spectra of compound **2b** in solution (blue dotted lines) and fibrous state (red straight lines). The xerogel exhibits narrow bathochromic shift (499 nm) in aggregated state attributed to the head-to-tail *J*-aggregate formation.

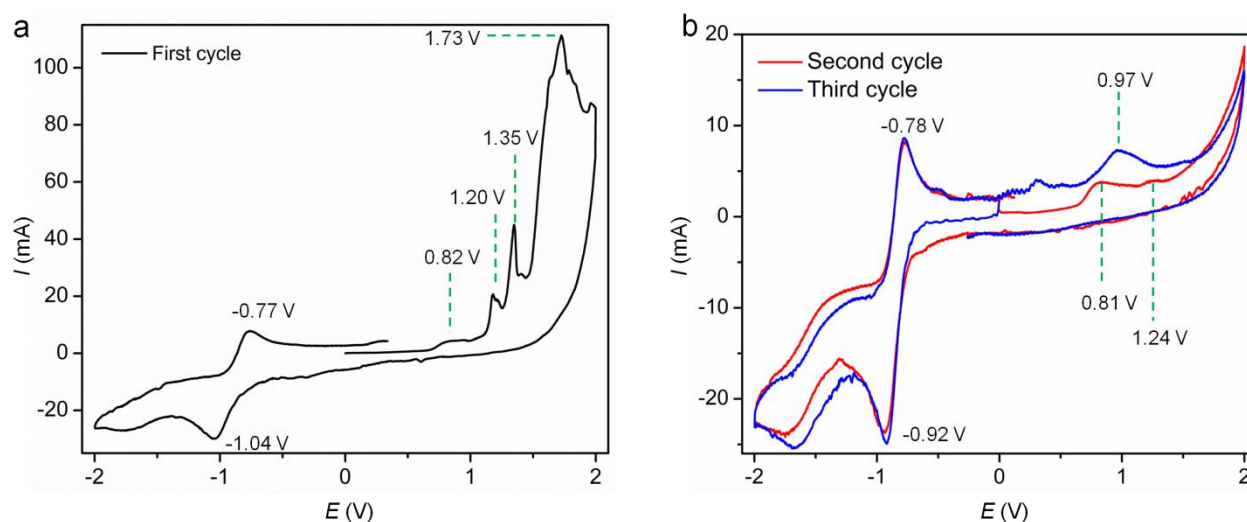


Fig. S11 Cyclic voltammograms of compound **2b** in fibrous state obtained by drop-casting DMF solution (0.2 mM, 10 μ L) of **2b** on the working electrode. (a) First cycle at the scan rate of 100 mVs^{-1} . (b) Second and third cycles at 50 mVs^{-1} .

Cyclic voltammetry carried out on xerogel **2b** in anhydrous acetonitrile by drop-casting DMF solution on glassy carbon electrode revealed irreversible oxidation peaks and one prominent reversible reduction peak. The irreversibility in oxidation is conspicuous with complete absence of corresponding cathodic reduction. The first cycle carried out at 100 mVs^{-1} showed the presence of at least four anodic oxidation peaks with E_{pa} values of 0.82V, 1.20 V, 1.35 V and 1.73 V (Fig. S11a). The second cycle performed at 50 mVs^{-1} retained only first two peaks (E_{pa} = 0.81 V and 1.24 V) with reduced current density for the second peak (Fig. S11b). The third cycle performed at 50 mVs^{-1} displayed only one anodic oxidation peak (E_{pa} = 0.97 V) (Fig. S11b). The lowering in the number of peaks with every subsequent cycle could be attributed to loss of analyte from the working electrode to the solution upon undergoing oxidation. The analyte with higher oxidation states plausibly possess increased solubility, which could be the reason for disappearance of peaks. Nevertheless, the reduction peak ($E_{1/2\text{red}}$ = -0.85 V) was reversible and did not lose current density throughout.

Current Sensing Atomic Force Microscopy (Cs-AFM)

The sample was prepared by drop-casting 0.1 mM DMF solution (10 μ L) of **2b** on a single crystal silicon wafer having a thickness and resistivity of 675 ± 25 μ m and $0.001 - 0.005$ Ω cm, respectively, at room temperature. The nanofibres were obtained upon slow evaporation of the solvent on the wafer and were subjected to Cs-AFM. Conductance measurements were carried out at different regions of the fibres where the current densities were high. Conductivity (σ) is calculated using the equation⁴

$$\sigma_{rt} = d/(A_t R) \text{ Scm}^{-1}$$

Where σ_{rt} is the conductivity at room temperature, and d is the average thickness of the fibres in the measured regions (~ 100 nm). A_t is the area of the C-AFM probe, which was in contact with the surface. A_t was calculated as πr^2 , assuming a contact radius between tip and sample to be 70 nm. R is the resistance of the sample, and $1/R$ was obtained by calculating the linear regression slope of I - V curve.

Linear regression slopes ($1/R$) obtained at three different regions and their corresponding conductivity:

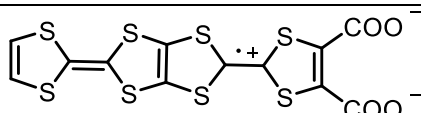
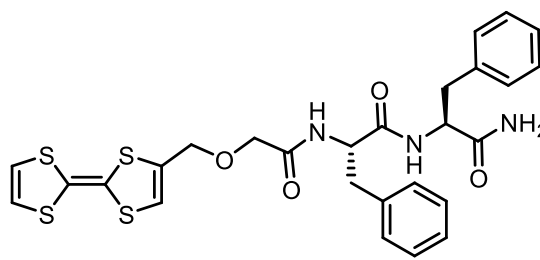
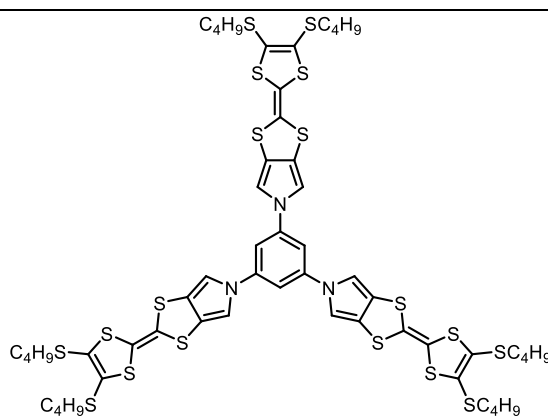
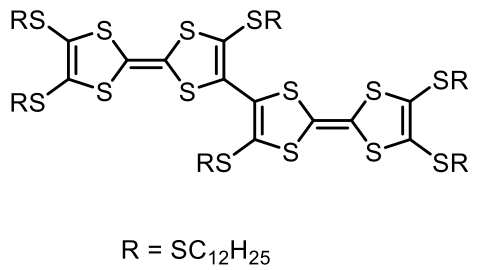
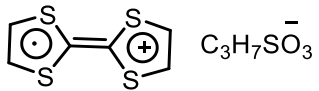
Region 1: $1/R = (2.22526 \pm 0.04824) \times 10^{-9}$ S; $\sigma_{rt} = 0.1445 \pm 0.0031$ mScm⁻¹

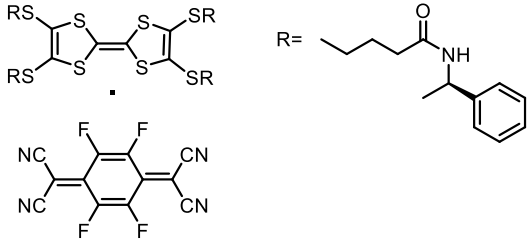
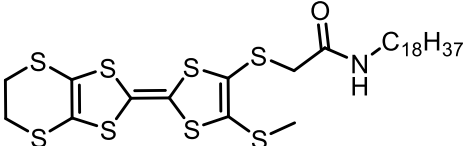
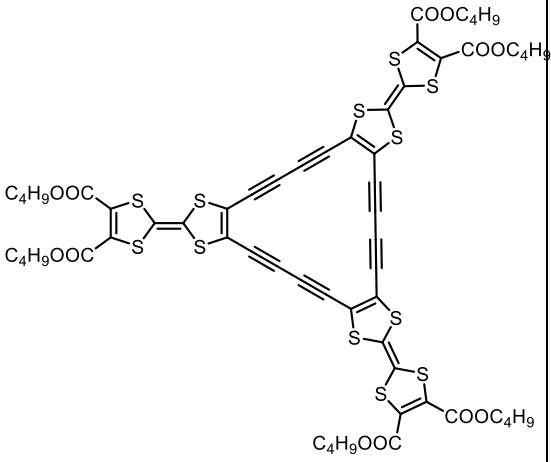
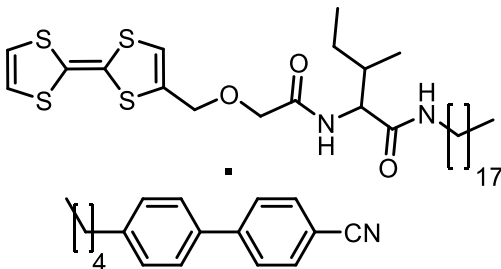
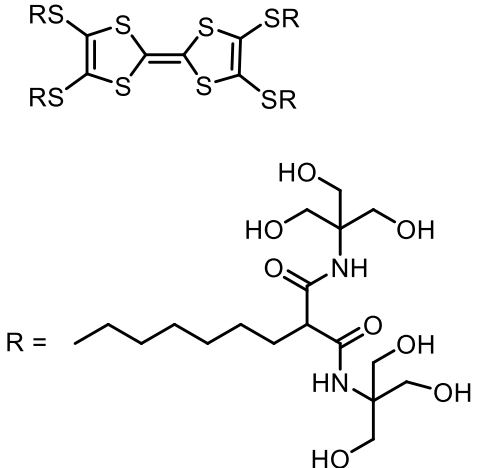
Region 2: $1/R = (2.26297 \pm 0.04541) \times 10^{-9}$ S; $\sigma_{rt} = 0.1469 \pm 0.0029$ mScm⁻¹

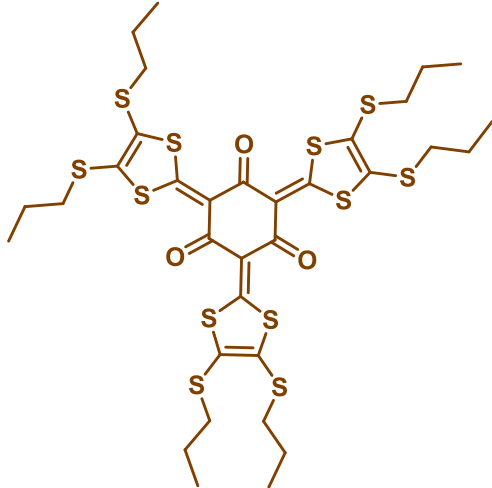
Region 3: $1/R = (2.25267 \pm 0.04622) \times 10^{-9}$ S; $\sigma_{rt} = 0.1463 \pm 0.0030$ mScm⁻¹

$$\text{Avg. } \sigma_{rt} = 0.1459 \pm 0.0030 \text{ mScm}^{-1}$$

Table S5. Comparison of conductivities reported at room temperature of various TTF derivatives forming 1D self-assembled structures.

Sl. No.	Molecular Structure	Sampling	Conductivity (S cm ⁻¹)	Reference
1		Compressed bulk solid	530	<i>Nat. Mater.</i> , 2017, 16 , 109
2		Undoped fibres TCNQ doped fibres	1.9×10^{-10} 3.6×10^{-4}	<i>Langmuir</i> 2014, 30 , 12429
3		Doped crystal Doped fibre Amorphous film	1.8×10^{-2} 1.9×10^{-2} 2.5×10^{-3}	<i>Org. Lett.</i> 2011, 13 , 3896
4	 R = SC ₁₂ H ₂₅	Undoped rods Doped with iodine/bromine vapors	1×10^{-6} $1.1\text{-}1.4 \times 10^{-4}$	<i>Tetrahedron Lett.</i> 2010, 51 , 679
5		Films of nanofibres	25.6×10^{-3}	<i>Langmuir</i> 2009, 25 , 6929

6		CT fibres (point contact current- imaging AFM)	$(7.0 \pm 3.0) \times 10^{-4}$	<i>Chem. Asian J.</i> 2009, 4 , 1474
7		Iodine doped pellet of fibres	$3-5 \times 10^{-3}$	<i>Angew. Chem. Int. Ed.</i> 2007 , <i>46</i> , 238
8		Undoped pellets of fibres Iodine doped pellets of fibres	$< 3 \times 10^{-6}$ $> 3 \times 10^{-3}$	<i>Org. Lett.</i> 2006 , <i>8</i> , 1917
9		Fibrous aggregates on silicon wafer	$< 3 \times 10^{-10}$ (undoped) 3×10^{-5} (iodine doped for 1 week) 1×10^{-5} (TCNQ doping)	<i>J. Am. Chem. Soc.</i> 2005 , <i>127</i> , 14769
10		Iodine doped film	$\sim 10^{-4}$	<i>Eur. J. Org. Chem.</i> 2003 , 3562

11		Undoped fibres (Cs-AFM)	0.15×10^{-3}	<i>This Work</i>
----	---	----------------------------	-----------------------	------------------

References

1. N. Svenstrup and J. Becher, *Synthesis*, 1995, **1995**, 215.
2. N. Godbert, A. Crispini, M. Ghedini, M. Carini, F. Chiaravalloti and A. Ferrise, *J. Appl. Crystallogr.*, 2014, **47**, 668.
3. A. K. Yadav, B. Pradhan, H. Ulla, S. Nath, J. De, S. K. Pal, M. N. Satyanarayan and A. S. Achalkumar, *J. Mater. Chem. C*, 2017, **5**, 9345.
4. S.-S. Chang and C.-G. Wu, *J. Phys. Chem. B*, 2005, **109**, 18275.